

## **Letter to the Editor of the ACP Manuscript “An estimation of the $^{18}\text{O}/^{16}\text{O}$ ratio of UT/LMS ozone based on artefact CO in air sampled during CARIBIC flights” by S. Gromov and C. A. M. Brenninkmeijer**

S. Gromov (on behalf of all authors)

Correspondence to: S. Gromov ([sergey.gromov@mpic.de](mailto:sergey.gromov@mpic.de))

Dear Dr. Kaiser,

We are very grateful for your great attention to this work and constructive comments that helped us to improve the quality of this manuscript significantly. Following your suggestions, we have prepared the revised version (please, find the pages with mark-up at the end of this letter). We have addressed all your comments (shown below italicised), on a few of them we have comments or different opinion, as we discuss in the following.

We appreciate very much the time you spent for editing this paper.

Best regards,

Sergey Gromov

### **Major points:**

#### *1) Contamination kinetic framework: <...>*

We are not going to carry on further polemics with the Editor who perennially tries to interpret a conceptual expression  $A \rightarrow B \rightarrow C$

as a strict chemical equation (besides that we have never stated that Eq. (A1) is one). We are grateful to the Editor for spending his precious time on enlightening us on textbook kinetics behind which, however, the discussion based on misinterpreted Eq. (A1) has nevertheless no sense. On the other hand, we admit that a mix-up of terms and formulations occurred, which inevitably impedes the Reader in understanding of what we have done. Ultimately, we find that we have rather used improper terminology than the kinetic apparatus, for which we sincerely apologise. We therefore decided to recast the “kinetic framework” (also renaming it to “contamination assessment” for clarity and leaving out any conceptual expressions, *i.e.* Eqs. (A1) and (A2)), as described below. Furthermore, restating the grounds of the kinetic apparatus we use, we are lucky to return to IUPAC definitions and conclude that Eqs. (A2) and (A3) in essence formulate the macroscopic rate of reaction (IUPAC “Gold book”, <http://dx.doi.org/10.1351/goldbook.O04322>), with  $K$  and  $\kappa$  being the partial orders of reaction with respect to concentrations of X and  $\text{O}_3$ , respectively, and  $k_c$  in our regression analysis being the so-called “observed” rate coefficient which determines the chemical flux of artefact CO. In the revised version of Appendix A we also better emphasise the set of assumptions involved, namely: (i) reaction time varies negligibly, (ii) changes to abundances of other reactants (if there are any) are negligible, and (iii) changes to other important parameters like temperature, pressure, flight time, *etc.* have no discernible effect on the amount of artefact CO produced. Finally, we state that merely a regression analysis was done.

*The “kinetic” framework is further compromised by the injudicious mixing of mole fractions and number densities. You state that the units match on both sides of your equations, but they don't in case of equations (A2) and (A3). E.g., in case of A3, the term  $[\text{O}_3]^\kappa$  has units of  $(\text{cm}^{-3})^{(2.06)} = \text{cm}^{-6.18}$ .*

In case of Eq. (A2), it is stated (ll. 367–368): “... (abundances in number density units are used)”. Eq. (A3) inherits its units from Eq. (A2) being a reduced form of it. Furthermore, we state (ll. 380–382): “... the product  $(\lambda_{\text{O}_3} k_c \tau_c)$  that proportionates the CO contamination strength and  $[\text{O}_3]$  is found to be  $(5.19 \pm 0.12) \cdot 10^{-5}$  mol/nmol ( $\pm 1\sigma$ , adj.  $R^2 = 0.83$ , red.  $\chi^2 = 4.0$ ; mole fraction units are used here for convenience).”

We explicitly state that, for convenience of the Reader,  $[O_3]$  (mole fraction of ozone) is to be used with this factor to quantify the CO contamination strength (also in mole fraction units). That is, by multiplying  $[O_3]^2$  (nmol/mol)<sup>2</sup> by  $(5.19 \pm 0.12) \cdot 10^{-5}$  (mol/nmol) the resulting value is to be in (nmol/mol)<sup>2</sup>  $\times$  (mol/nmol) = (nmol/mol), *i.e.* in mole fraction units. Such conversion is possible because the pressure and temperature variations do not result in significant variations of air density at the C1 sampling conditions. We neither find “injudicious mixing of mole fractions and number densities” here nor understand how this can “compromise the “kinetic” framework”.

*I am unable to see how you derive a dependence of the CO artefact formation rate on the squared ozone number density.*

*This leaves the empirical regression equation to justify the apparent dependence of the artefact mixing ratio on the (approximate) square of the O3 mixing ratio. However, looking at Fig. 1d, I'd suggest that a linear fit would give almost as good a fit as power fit (to the power of 2.06). In addition, a linear fit could be more directly related to a kinetic mechanism (as suggested above).*

We appreciate Editor’s ability to infer goodness of fit by contemplating the data with a naked eye. Being not confident of applying this method ourselves, however, we used the conventional apparatus (*viz.*  $R^2$  and reduced  $\chi^2$  statistic), as duly communicated in Appendix A. We also remain certain, that it is clear to the Editor that the regression analyses were performed sequentially. That is, firstly the expression in Eq. (A3) is regressed with respect to two parameters, namely the product  $(\lambda_{O_3} \cdot k_c \tau_c)$  and  $\kappa$ , which yields the least value of reduced  $\chi^2$  at  $\kappa$  of  $(2.06 \pm 0.38)$ . Secondly, taking (assuming)  $\kappa = 2$  the regression of the product  $(\lambda_{O_3} \cdot k_c \tau_c)$  is done. In this step we also ascertain that regression yields the least reduced  $\chi^2$  value at  $\kappa = 2$ , in contrast to  $\kappa$  being equal any other integer number.

To summarise, we propose the following amendment of Appendix A (and looking forward to your kind suggestions for improvement):

### Appendix A. Contamination assessment

We quantify the C1 CO contamination strength (denoted  $[CO]_c$ , obtained by discriminating the C1 outliers from respective C2 data) in a sequence of regression analyses. We foremost ascertain that no other species or operational parameter (*e.g.* temperature, pressure, flight duration, season, latitude, time of day, *etc.*) measured in C1 appear to determine (*e.g.*, systematically correlate with)  $[CO]_c$ , except that for  $[O_3]$ . We hypothesise therefore that a production of artefact CO molecules was initiated by  $O_3$  (via either its decomposition or a reaction with an unknown educt) and proceeded with incorporation of carbon (donated by some carbonaceous species X) and oxygen (donated by  $O_3$  or its derivatives) atoms into final CO. Despite that neither the actual reaction chain nor its intermediates are known, it is possible to describe the artefact CO component produced (hereinafter curly brackets  $\{\}$  denote number densities) as

$$\{CO\}_c = \lambda_{O_3} \nu \tau_c, \quad (A1)$$

where the yield  $\lambda_{O_3}$ , a diagnostic quantity, relates the amount of artefact CO molecules produced to the total number of  $O_3$  molecules consumed in the system,  $\tau_c$  denotes the reaction time (period throughout which sampled air is exposed to contamination), and  $\nu$  stands for the overall rate of the reaction chain. The latter, being regarded macroscopically (empirically), is parameterised to account for the order of reaction chain rate with respect to hypothesised reactants (McNaught and Wilkinson, 1997) as

$$\nu = k \{X\}^K \{O_3\}^\kappa, \quad (A2)$$

where  $\kappa$  and  $K$  are the partial orders with respect to X and  $O_3$  number densities, respectively, and  $k$  is the rate coefficient. Here it is implied that changes to  $\{X\}$  and  $\{O_3\}$  are negligible throughout the exposure time  $\tau_c$  (typically  $< 0.1$  s for C1 sample line). As stated above, we find that variations in  $\{CO\}_c$  correlate exclusively with variations in  $\{O_3\}$ , hence Eq. (A2) can be reduced by assuming constancy of  $\{X\}$  and  $K$  to:

$$\nu_c = k_c \{O_3\}^\kappa. \quad (A3)$$

Here,  $k_c = k \{X\}^K$  (often referred to as pseudo-first-order or “observed” rate coefficient) quantifies the rate of reaction chain exclusively propelled by  $O_3$ . Finally, using Eqs. (A1) and (A3), the artefact  $\{CO\}_c$  component is expressed as

$$\{CO\}_c = b \cdot \{O_3\}^\kappa, \quad b = \lambda_{O_3} k_c \tau_c \quad (A4)$$

where the constant proportionality factor  $b$  integrates the influence of the unknown (and as we explicate below, likely invariable)  $\{X\}$ ,  $k$ ,  $K$  and  $\tau_c$ .

Eq. (A4) defines the regression expression using which we attempt to fit the values of  $\{\text{CO}\}_c$  as a function of  $\kappa$ ,  $\{\text{O}_3\}$  and  $b$ . In the first regression iteration we keep both  $\kappa$  and  $b$  as free parameters, which provides best approximation at  $\kappa = 2.06 \pm 0.38$ , suggesting reactions of two  $\text{O}_3$  molecules in case elementary reactions constitute the reaction mechanism, or two elementary steps involving  $\text{O}_3$  or its derivatives in case a stepwise reaction is involved (McNaught and Wilkinson, 1997). In a subsequent regression iteration we set  $\kappa = 2$ , which yields better (as opposed to the first iteration) estimate of  $b$  of  $(5.19 \pm 0.12) \cdot 10^{-5}$  mol/nmol ( $\pm 1\sigma$ , adj.  $R^2 = 0.83$ , red.  $\chi^2 = 4.0$ ; here the equivalent value in mole fraction units is quoted for the convenience of relating fitted  $[\text{CO}]_c$  and  $[\text{O}_3]^2$ ). At last, we ascertain that the best regression results are obtained particularly at  $\kappa = 2$ , as indicated by the regression statistic ( $R^2$  and  $\chi^2$ ) that asymptotically improves when a set of regressions with neighbouring (*i.e.* below and above 2) integer values of  $\kappa$  is compared. The low uncertainty (within  $\pm 3\%$ ) associated with the estimate of  $b$  confirms an exclusive dependence of the contamination source on the  $\text{O}_3$  mixing ratio, as well as much similar reaction times  $\tau_c$ . The regressed value of  $[\text{CO}]_c$  as a function of  $[\text{O}_3]$  is presented in Fig. 1 (d) (solid line). It is possible to constrain the overall yield  $\lambda_{\text{O}_3}$  of CO molecules in the artefact source chain to be between 0.5 and 1, comparing the magnitude of  $[\text{CO}]_c$  to the discrepancy between the  $[\text{O}_3]$  measured in C1 and C2 ( $\pm 20$  nmol/mol, taken equal to the  $[\text{O}_3]$  bin size owing to the  $\text{N}_2\text{O}-\text{O}_3$  and  $\text{H}_2\text{O}-\text{O}_3$  distributions matching well between the datasets). Lower  $\lambda_{\text{O}_3}$  values, otherwise, should have resulted in a noticeable (*i.e.*, greater than 20 nmol/mol) decrease in the C1  $\text{O}_3$  mixing ratios with respect to the C2 levels.

2) Please do not deviate unnecessarily from established nomenclature, *e.g.* "abundance" is not a defined concentration quantity and should not be used as such. It is only defined in terms of isotopic abundances. Please stick with the terms "mixing ratio" (and explain at some point that you understand this to mean "mole fraction") and, if required, "number density". You might find the following paper of interest:

Cvitaš T (1996) *Quantities describing compositions of mixtures Metrologia:35 doi:10.1088/0026-1394/33/1/5*

To avoid confusion, please use the same symbol for a specific quantity throughout the manuscript. For example, you use both square brackets and "C" for mixing ratios. Please use only one of these two. Also, if you use square brackets to denote mixing ratios, please do not also use this for number densities. Note that the IUPAC Green Book recommends the symbol "y" for mole fractions in gaseous mixtures and the symbol "C" for number densities (<http://media.iupac.org/publications/books/gbook/IUPAC-GB3-2ndPrinting-Online-22apr2011.pdf>).

We replace all "C" with equivalent "[CO]" terms throughout the revised manuscript. For the number densities (used only in Appendix A) we prefer to use curly brackets, *e.g.* "{CO}".

3) Please decide on your preferred delta notation and stick with it. If you were to follow IUPAC recommendations, you would have to write  $\delta(18\text{O}, \text{O}_3)$ ,  $\delta(18\text{O}, \text{CO})$ , etc. However, I acknowledge that, unfortunately, many isotope geochemists have adopted the incorrect notation  $\delta 18\text{O}(\text{O}_3)$  etc., perhaps because they mixed up the physical quantity symbol delta with a mathematical operator (which, however, would also be wrong because a mathematical operator cannot be applied to a chemical symbol).

We prefer to stick with the " $\delta^{18}\text{O}(\text{O}_3)$ " notation, as we acknowledge that the vast majority of literature using delta notation sticks with it, in contrast to the IUPAC recommendations.

4) Please remove tilde signs and round values adequately and/or give uncertainties, as appropriate. In any case, the tilde sign should not be used to indicate approximations; the correct symbol is " $\approx$ " (two wavy lines one above the other). However, since very few of the values mentioned in the paper are exact, the approximation sign is almost always redundant and would be best omitted. Instead the corresponding value should be given with an appropriate number of significant figures according to its uncertainty.

We have corrected all occurrences according to your kind suggestions.

### **Technical corrections:**

5: A photochemical nature is not ascertained because no detailed process studies or kinetic modelling has been undertaken. Photochemistry is unlikely in the (largely) dark pipes of the sampling system. Rather, you "suggest that the magnitude of the artefact is proportional to the square of the ozone mixing ratio".

Correct. We change it to "(ii) ascertain the chemical nature and quantify the strength of the contamination, and ...".

8: Replace "signature" with "delta" and 18O/16O ratios with delta18O. Replace "unambiguously" with "likely".

We use "isotope composition" instead of "isotope signature".

14: Delta needs to be in italics.

We are certain this will be taken care of during the typesetting of the manuscript (if it comes to that) according to the ACP conventions (these imply italicised delta, as far as we know).

93: Add "in situ" after C2 for clarity.

Added. In Sect. 2.1 (above) we already state that, however.

99: "in NH tropospheric emissions" (otherwise this would be a tautology)

We see no tautology here. The CO variations result from mixing of the little varying stratospheric [CO] and largely varying tropospheric [CO]. It is the result of mixing we discuss here. Besides, variations in tropospheric [CO] are *by far* more strongly determined by the presence of hydroxyl radical than by the variations in emissions.

102: "in C1 and C2 [CO], for [O3] > 400 nmol/mol the C1 CO mixing ratios [...]"

This comment is unclear to us. We describe continuous changes in [CO] with increasing [O<sub>3</sub>], this will change the meaning of the sentence to something we do not intend to state.

104: "In the 580-600 nmol/mol [O3] bin"

This comment is unclear to us. We describe to what [CO] in C1 one observes in particular bin (around 580 nmol/mol of [O<sub>3</sub>]), this will change the meaning of the sentence to something we do not intend to state.

105: "accommodates and extra 14 nmol/mol"

Here we meant that this [CO] contains extra 15 nmol/mol as compared to average C2 value. We adjust the statement accordingly.

160-162: This sentence duplicates the message of the previous one and can be deleted.

Please explain. The statements "[CO] from WAS and *in situ* measurements correlate well" and "anomalies in both [CO] and δ<sup>18</sup>O(CO) manifest functions of [O<sub>3</sub>]" do not appear duplicate to us.

171: This ratio appears to be wrong and should be 600:70 based on the values given here.

Rather the ratio of 600:70 appears to be wrong.

Taking the weighted sum of 700 (85%) and 60 (15%), one receives  $700 \cdot 0.85 + 60 \cdot 0.15 = 604$ . Taking the weighted sum of 24 (85%) and 125 (15%), one receives  $24 \cdot 0.85 + 125 \cdot 0.15 = 39.15$ . This is 4% and 2% off from the quoted 580 and 40, respectively. The ratio 600:70 implies the resulting [CO] about 80% higher than the correct value.

To be more precise, we adjust the figures accordingly:

For example, mixing of two air parcels in a 16%:84% proportion (by moles of air) with typical [O<sub>3</sub>]:[CO] of 700:24 (stratospheric) and 60:125 (tropospheric), respectively, yields an integrated composition with [O<sub>3</sub>]:[CO] of 598:40 which indeed corresponds to C1 data (this case is exemplified by the mixing curve in Fig. 1).

184: This sentence does not make sense. [H2O] cannot witness [CO]:[O3] ratios. Please change or delete the entire sentence from l. 183 to 185 as it does not appear to add any information.

Thank you, we change "[CO]:[O<sub>3</sub>]" to "[O<sub>3</sub>]:[H<sub>2</sub>O]" for clarity.

197-200: This sentence is unclear - is this meant to be a contradiction, confirmation, fact, assumption, hypothetical calculation or what?

We change it to:

Our simulations of the 'translational mixing' effects confirm that the actual C2 CO–O<sub>3</sub> distribution in the region of interest ([O<sub>3</sub>] of 540–620 nmol/mol) remains insensitive to averaging intervals of up to 300 s.

206: Replace "abundance" with "mixing ratio" and change "imply" to "suggest". Why photochemical? O<sub>3</sub> could reaction in the dark as well?

We change it to "O<sub>3</sub>-mediated production of CO took place".

223: Please delete "Practically" and change "resort" to "use". The Keeling plot itself does *not* require an estimate of [CO]<sub>c</sub>; however, your data selection criterion (for delta\_true) does. Please change this sentence accordingly.

Perhaps, the Editor has misunderstood the message of the sentence. Here we emphasise that we can employ the MM using solely the estimate of the contamination strength (*i.e.*, the amount of molecules admixed to the reservoir with some initial composition). Furthermore, do you imply that using the Keeling plot one does not require to know the amount of molecules admixed into a reservoir with known starting composition? (It obviously would be nonsense, of course, perhaps we did not understand your comment?)

227: Please break this into two equations and number the equations. Indices should not be italics. The symbol C should be replaced with [CO] for consistency (or "y" if you adopt IUPAC symbols; see comment 2 above).

See our answer to comment 2) above. Regarding the italics, see our answer to l. 14 above.

253: The symbol  $\delta_c$  has not been defined. For consistency, this should be  $\delta_{13C_c}(CO)$ , or, following conventional symbol and index notation,  $\delta_c(13C, CO)$ .

The Editor contradicts himself here. In the previous version of the manuscript we used a consistent notation using indices to distinguish  $\delta_c$  for <sup>13</sup>C and <sup>18</sup>O, which the Editor requested to remove (see the comment on l. 227 of the previous version). Since distinguishing different  $\delta_c$ ,  $\delta_a$  and  $\delta_i$  variables is obviously necessary we return to the previous notation, *e.g.*  $\delta_c^{13}$  and  $\delta_c^{18}$ .

348: Add "in combination with an empirical parameterisation of the [CO] artefact in terms of the O<sub>3</sub> mixing ratio" after brackets, followed by "to single out ..."

We would like to keep the current formulation, as we already make a statement above (ll. 345–346) on the quantification of the artefact CO production.

Fig. 6: The x-axis label should be "MM", not MMA. The legend labels should be  $\delta_{18O_c}(O_3)$  and  $\delta_{13C_c}(O_3)$ ; also in the caption.

We change the labels to  $\delta_c^{18}$  and  $\delta_c^{13}$ , respectively, that are clearly associated with calculations with the MM. This also allows to avoid somewhat confusing  $\delta^{13C_c}(O_3)$  (the carbon isotope ratio from O<sub>3</sub> makes no sense here).

613: " $\delta_t^{18O}$ " should be deleted.

Perhaps, the Editor did not understand this statement. Different  $R^2$  values are obtained for different signatures being regressed, *i.e.* for  $\delta_c^{18}$  and  $\delta_c^{13}$ . Here we emphasise the pair of  $\delta_c^{13}$  values encircled corresponds to the pair of best-guessed  $\delta_c^{18}$  values which are obtained with highest  $R^2$  value.

# An estimation of the $^{18}\text{O}/^{16}\text{O}$ ratio of UT/LMS ozone based on artefact CO in air sampled during CARIBIC flights

S. Gromov<sup>1</sup>, C. A. M. Brenninkmeijer<sup>1</sup>

<sup>1</sup> Max Planck Institute for Chemistry, Mainz, Germany

Correspondence to: S. Gromov ([sergey.gromov@mpic.de](mailto:sergey.gromov@mpic.de))

## Abstract

An issue of  $\text{O}_3$ -driven artefact production of CO in the upper troposphere/lowermost stratosphere (UT/LMS) air analysed in the CARIBIC-1 project is being discussed. By confronting the CO mixing and isotope ratios obtained from different analytical instrumentation, we (i) reject natural/artificial sampling and mixing effects as possible culprits of the problem, (ii) ascertain the chemical nature and quantify the strength of the contamination, and (iii) demonstrate successful application of the isotope mass-balance calculations for inferring the isotope composition of the contamination source. The  $\delta^{18}\text{O}$  values of the latter indicate the oxygen likely being inherited from  $\text{O}_3$ . The  $\delta^{13}\text{C}$  values hint at reactions of trace amounts of organics with stratospheric  $\text{O}_3$  that could have yielded the artificial CO. While the exact contamination mechanism is not known, it is clear that the issue pertains only to the earlier (first) phase of the CARIBIC project. Finally, estimated UT/LMS ozone  $\delta^{18}\text{O}$  values are lower than those observed in the stratosphere within the same temperature range, suggesting that higher pressures (240–270 hPa) imply lower isotope fractionation controlling the local  $\delta^{18}\text{O}(\text{O}_3)$  value.

## 1 Introduction

[1] Accurate determination of the atmospheric carbon monoxide (CO) mixing ratio based on the collection of air samples depends on the preservation of the mixing ratio of CO inside the receptacle, from the point of sampling to the moment of physicochemical analysis in a laboratory. A well known example in our field of research is the filling of pairs of glass flasks at South Pole

Deleted: /

Deleted: R

Deleted: A

Deleted: photo

Deleted: effect in a general

Deleted: kinetic framework

Deleted: D

Deleted: the

Deleted: signature

Deleted:  $^{16}\text{O}$  ratios

Deleted: unambiguously

Deleted:  $^{12}\text{C}$  ratios

Deleted: ample

Deleted:  $^{18}\text{O}$  ratios

Deleted: LMS

Deleted: Successful

Deleted: content

37 Station for analysis at NOAA in Boulder, Colorado, USA (Novelli *et al.*, 1998). There, the du-  
38 plicate air sampling allowed for a degree of quality control which in view of the long transit  
39 times, especially during polar winter, was a perhaps not perfect, but certainly a practical meas-  
40 ure. Here we deal with a different case: Using aircraft-based collection of very large air samples  
41 rendered duplicate sampling unpractical, yet analyses could be performed soon after the sam-  
42 pling had taken place because of the proximity of the aircraft's landing location to the laborato-  
43 ry involved. A presumption of the analytical integrity of the process was that the growth of CO  
44 in receptacles is gradual and takes its time. Reminding Thomas Henry Huxley's statement, "The  
45 great tragedy of Science – the slaying of a beautiful hypothesis by an ugly fact", it turned out,  
46 however, that for air we collected in stainless steel tanks in the upper troposphere/lowermost  
47 stratosphere (UT/LMS) higher CO values were measured in the laboratory than measured  
48 *in situ* during the collection of these air samples. Moreover, measurement of the stable oxygen  
49 isotopic composition of CO from these tanks revealed additional isotopic enrichments in  $^{18}\text{O}$  of  
50 10‰ or more. It was soon realised that this phenomenon was due to the formation of CO in  
51 these tanks and/or possibly in the sampling system and inlet tubing used, by reactions involving  
52 ozone (Brenninkmeijer *et al.*, 1999).

53 [2] Unexpectedly high  $^{18}\text{O}/^{16}\text{O}$  ratios in stratospheric ozone ( $\text{O}_3$ ) were discovered by Konrad  
54 Mauersberger using a balloon-borne mass spectrometer (Mauersberger, 1981), which has trig-  
55 gered a series of theoretical and experimental studies on atmospheric  $\text{O}_3$  heavy isotope enrich-  
56 ments (see, *e.g.*, Schinke *et al.* (2006) for a review). In view of the advances in theoretical and  
57 laboratory studies on the isotopic composition of  $\text{O}_3$  atmospheric measurements are welcome,  
58 they do however form a challenge. In the stratosphere  $\text{O}_3$  number concentrations are high, but  
59 the remoteness of the sampling domain is a problem. In the troposphere, low  $\text{O}_3$  number densi-  
60 ties are the main obstacle, as indicated by few experiments performed to date  
61 (Krankowsky *et al.*, 1995; Johnston and Thiemens, 1997; Vicars and Savarino, 2014). Never-  
62 theless, recent analytical improvements, namely the use of an indirect method of reacting at-  
63 mospheric  $\text{O}_3$  with a substrate that can be analysed for the isotopic composition of the  
64  $\text{O}_3$ -derived oxygen (Vicars *et al.*, 2012), has greatly improved our ability to obtain information  
65 on the  $\text{O}_3$  isotopic composition.

66 [3] Although the increase of CO concentrations in air stored in vessels is a well recognised  
67 problem, to our knowledge a specific  $\text{O}_3$ -related process has not been reported yet. Here we dis-  
68 cuss this phenomenon and turn its disadvantage into an advantage, namely that of obtaining an  
69 estimate of the oxygen isotopic composition of  $\text{O}_3$  in the UT/LMS, an atmospheric domain not

Deleted: is abundant

Deleted: concentrations

Deleted: valid

73 yet covered by specific measurements. The air samples we examine in this study were collected  
74 onboard a passenger aircraft carrying an airfreight container with analytical and air/aerosol  
75 sampling equipment on long distance flights from Germany to South India and the Caribbean  
76 within the framework of the CARIBIC project (Civil Aircraft for the Regular Investigation of  
77 the atmosphere Based on an Instrument Container, <http://www.caribic-atmospheric.com>).

## 78 2 Experimental and results

### 2.1 Whole air sampling

79 [4] CARIBIC-1 (Phase #1, abbreviated hereafter “C1”) was operational from November 1998  
80 until April 2002 using a *Boeing* 767-300 ER operated by LTU International Airlines  
81 (Brenninkmeijer *et al.*, 1999). Using a whole air sample (WAS) collection system, twelve air  
82 samples were collected per flight (of 8–10 hours duration at cruise altitudes of 10–12 km) in  
83 stainless steel tanks for subsequent laboratory analysis of the mixing ratios (*i.e.* mole fractions),  
84 of various trace gases, including  $^{14}\text{CO}$ . Large air samples were required in view of the ultra-low  
85 number density of this mainly cosmogenic tracer (10–100 molecules  $\text{cm}^{-3}$  standard temperature  
86 and pressure (STP), about 0.4–4 amol/mol). Hereinafter STP denotes dry air at 273.15 K,  
87 101325 Pa. Each C1 WAS sample (holding 350 litres of air STP) was collected over 15–20 min  
88 intervals representing the number density-weighted average of the compositions encountered  
89 along flight segments of about 250 km. The overall uncertainty of the measured WAS CO is  
90 less than  $\pm 1\%$  for the mixing ratio and  $\pm 0.1\%/\pm 0.2\%$  for  $\delta^{13}\text{C}(\text{CO})/\delta^{18}\text{O}(\text{CO})$ , respectively  
91 (Brenninkmeijer, 1993; Brenninkmeijer *et al.*, 2001). Isotope compositions are reported  
92 throughout this manuscript using the so-called delta value  $\delta = (R/R_{\text{st}} - 1)$  relating the ratio  $R$  of  
93 rare ( $^{13}\text{C}$ ,  $^{18}\text{O}$  or  $^{17}\text{O}$ ) over abundant isotopes of interest to the standard ratio  $R_{\text{st}}$ . These are Vien-  
94 enna Standard Mean Ocean Water for  $^{18}\text{O}/^{16}\text{O}$  (Gonfiantini, 1978; Coplen, 1994) and  $^{17}\text{O}/^{16}\text{O}$   
95 (Assonov and Brenninkmeijer, 2003), and Vien-  
96 enna Pee Dee Belemnite for  $^{13}\text{C}/^{12}\text{C}$  (Craig, 1957),  
97 respectively. As we mention above, the oxygen isotope composition of the CO present in these  
98 WAS samples was corrupted, in particular when  $\text{O}_3$  levels were as high as 100–600 nmol/mol.

99 [5] CARIBIC-2 (Phase #2, referred to as “C2”) started operation in December 2004 with a  
100 Lufthansa *Airbus* A340-600 fitted with a new inlet system and air sampling lines, including per-  
101 fluoroalkoxy alkane (PFA) lined tubing for trace gas intake (Brenninkmeijer *et al.*, 2007). No  
102 flask CO mixing/isotope ratio measurements are performed in C2.

Deleted: abundances

Deleted: abundance

Deleted: 0

Deleted: 00

Deleted: (

Deleted: )

Deleted: within

Deleted: integral

Deleted: -

Deleted: of  $2005.20 \times 10^{-6}$

Deleted:  $386.72 \times 10^{-6}$  for

Deleted: -

Deleted: of  $11237.2 \times 10^{-6}$

Deleted: ic



## 2.2 On-line instrumentation

[6] In addition to the WAS collection systems, both C1 and C2 measurement setups include different instrumentation for on-line detection of [CO] and [O<sub>3</sub>] (hereinafter the squared brackets [] denote the mixing ratio of the respective species). *In situ* CO analysis in C1 is done using a gas chromatography (GC)-reducing gas analyser which provides measurements every 130 s with an uncertainty of ±3 nmol/mol (Zahn *et al.*, 2000). In C2, a vacuum ultraviolet fluorescence (VUV) instrument with lower measurement uncertainty and higher temporal resolution of ±2 nmol/mol in 2 s (Scharffe *et al.*, 2012) is employed. Furthermore, the detection frequency for O<sub>3</sub> mixing ratios, has also increased, viz., from 0.06 Hz in C1 to 5 Hz in C2 (Zahn *et al.*, 2002; Zahn *et al.*, 2012).

Deleted: abundance, i.e. concentration or

Deleted: ,

Deleted: , respectively

Deleted: abundances

## 2.3 Results

[7] When comparing the CO mixing ratios in relation to those of O<sub>3</sub> for C1 and C2, differences are apparent in the LMS, where C2 [CO] values are systematically lower. This is illustrated in Fig. 1 (a) which presents the LMS CO-O<sub>3</sub> distribution of the C2 *in situ* measurements overlaid with the C1 *in situ* and WAS data. The entire C1 CO/O<sub>3</sub> dataset is presented in Fig. 2. For the *in situ* CO datasets we calculated the statistics (Fig. 1 (b)) of the samples with respective O<sub>3</sub> mixing ratios clustered in 20 nmol/mol bins, i.e. the median and spread of [CO] as a function of [O<sub>3</sub>] analysed. The interquartile range, IQR, is used in the current analysis as a robust measure of the data spread instead of the standard deviation. The data exhibit large [CO] variations at [O<sub>3</sub>] below 400 nmol/mol that primarily reflect pronounced seasonal variations in the NH tropospheric CO mixing ratio. With increasing [O<sub>3</sub>], [CO] decreases to typical stratospheric values, and its spread reduces to mere 3.5 nmol/mol and less, as [O<sub>3</sub>] surpasses 500 nmol/mol. Despite the comparable spread in C1 and C2 [CO], from 400 nmol/mol of [O<sub>3</sub>] onwards the C1 CO mixing ratios start to level off, with no samples below 35 nmol/mol having been detected, whereas the C2 levels continuously decline. By the 580 nmol/mol O<sub>3</sub> bin, C1 [CO] of 39.7<sup>+0.7</sup><sub>-0.7</sub> nmol/mol contains some extra 15 nmol/mol compared to 25.6<sup>+1.7</sup><sub>-1.7</sub> nmol/mol typical for C2 values. Overall, at [O<sub>3</sub>] above 400 nmol/mol the conspicuously high [CO] is marked in about 200 *in situ* C1 samples, of which 158 and 69 emerge as statistically significant mild and extreme outliers, respectively, when compared against the number of C2 samples ( $n > 3 \cdot 10^5$ ). The conventions here follow Natrella (2003), i.e. ±1.5 and ±3 IQR ranges define the inner and outer statistical fences (ranges outside which the data points are considered mild and extreme outliers) of the C2 [CO] distribution in every O<sub>3</sub> bin, respectively. The statistics include the samples in bins with average

Deleted: abundances

Deleted: (

Deleted: )

Deleted: abundances

Deleted: (

Deleted: )

Deleted: abundance

Deleted: rising

Deleted: accommodates

Deleted: C2 statistics

Deleted: (

162 [O<sub>3</sub>] of 420–620 nmol/mol. None of C1 CO at [O<sub>3</sub>] above 560 nmol/mol agrees with the C2 ob-  
163 servations. Because the CO-O<sub>3</sub> distribution cannot have changed over the period in question, we  
164 find that an apparent relative excess CO of up to 55% justifies and investigation into sampling  
165 artefacts and calibration issues.

166 [8] Unnatural elevations in  $\delta^{18}\text{O}(\text{CO})$  from WAS measurements are also evident, as shown in  
167 Figs. 3 and 4. The large  $\delta^{18}\text{O}(\text{CO})$  elevations that reach beyond +16‰ are found to be propor-  
168 tional to the concomitant O<sub>3</sub> mixing ratios (denoted with colour) and are more prominent at  
169 lower [CO]. Lower  $\delta^{18}\text{O}(\text{CO})$  values, however, are expected based on our knowledge of UT/  
170 LMS CO sources (plus their isotope signatures) and available *in situ* observations (Fig. 3,  
171 shown with triangles), as elucidated by Brenninkmeijer *et al.* (1996) (hereafter denoted as  
172 “B96”). That is, the greater the proportion of stratospheric CO, the greater its fraction stemming  
173 from methane oxidation with a characteristic  $\delta^{18}\text{O}$  of 0‰ or lower (Brenninkmeijer and Röck-  
174 mann, 1997). This occurs because the CO sink at ruling UT/LMS temperatures proceeds more  
175 readily than its production, as the reaction of hydroxyl radical (OH) with CO, being primarily  
176 pressure-dependent, is faster than the temperature-sensitive reaction of OH with CH<sub>4</sub>. Further-  
177 more, as the lifetime of CO quickly decreases with altitude, transport-mixing effects take the  
178 lead in determining the vertical distributions of [CO] and  $\delta^{18}\text{O}(\text{CO})$  above the tropopause,  
179 hence their mutual relationship. This is seen from the B96 data at [CO] below 50 nmol/mol that  
180 line-up in a near linear relationship towards the end-members with lowest <sup>18</sup>O/<sup>16</sup>O ratios. These  
181 result from the largest share of the <sup>18</sup>O-depleted photochemical component and extra depletion  
182 caused by the preferential removal of C<sup>18</sup>O in reaction with OH (fractionation about +11‰ at  
183 pressures below 300 hPa, Stevens *et al.*, 1980; Röckmann *et al.*, 1998b).

184 [9] We are confident that the enhancements of C1 C<sup>18</sup>O originate from O<sub>3</sub>, whose large enrich-  
185 ment in <sup>18</sup>O (above +60‰ in  $\delta^{18}\text{O}$ , Brenninkmeijer *et al.*, 2003) is typical and found transferred  
186 to other atmospheric compounds (see Savarino and Morin (2012) for a review). In Fig. 3 it is al-  
187 so notable that not only the LMS compositions are affected but elevations of (3–10)‰ from the  
188 bulk  $\delta^{18}\text{O}(\text{CO})$  values are present in more tropospheric samples with [CO] of up to  
189 100 nmol/mol. These result from the dilution of the least affected CO-rich tropospheric air by  
190 CO-poor, however substantially contaminated, stratospheric air, sampled into the same WAS  
191 tank. Such sampling-induced mixing renders an unambiguous determination of the artefact  
192 source’ isotope signature rather difficult, because neither mixing nor isotope ratios of the ad-  
193 mixed air portions are known sufficiently well (see below).

Deleted: )

Deleted: levels

Deleted: by the difference

Deleted: (

Deleted: ),

Deleted: need to be scrutinised

Deleted: the

Deleted: <sup>18</sup>O ratios

Deleted: of

Deleted: departures

Deleted: abundances

Deleted: A rather different relationship

Deleted: is

Deleted: from

Deleted: Fig. 2

Deleted: more

Deleted: is

Deleted: of its local inventory is re-  
filled with the photochemical component

Deleted: signature

Deleted: ~

Deleted: outcompetes

Deleted: ~

Deleted: It is beyond doubt

Deleted: heavy oxygen

Deleted: Fig. 2

Deleted: ~

[10] Differences between the WAS and *in situ* measured [CO] – a possible indication that the  $\delta^{18}\text{O}(\text{CO})$  contamination pertains specifically to the WAS data – average at  $\bar{\Delta}(\text{WAS}-\textit{in situ}) = (5.3 \pm 0.2)$  nmol/mol ( $\pm 1$  standard deviation of the mean,  $n = 408$ ) and happen to be random with respect to any operational parameter or measured characteristic in C1, *i.e.* irrespective of CO or  $\text{O}_3$  abundances. The above mentioned discrepancy remained after several calibrations between the two systems had been performed, and likely results from the differences in the detection methods, drifts of the calibration standards used (see details in Brenninkmeijer *et al.*, 2001) and a short-term production of CO in the stainless steel tanks during sampling. The large spread of  $\Delta(\text{WAS}-\textit{in situ})$  of  $\pm 3.5$  nmol/mol ( $\pm 1\sigma$  of the population) ensues from the fact that the *in situ* sampled air corresponds to (2–4)% of the concomitantly sampled WAS volume, as typically 6–7 *in situ* collections of 5 s were made throughout one tank collection of 17–21 min. The integrity of the WAS CO is further affirmed by the unsystematic distribution of the artefact compositions among tanks (in contrast to that for  $\delta^{18}\text{O}(\text{CO}_2)$  in C1 discussed by Assonov *et al.*, 2009). Overall, the WAS and *in situ* measured CO mixing ratios correlate extremely well (adj.  $R^2 = 0.972$ , slope of  $0.992 \pm 0.008$  ( $\pm 1\sigma$ ),  $n = 408$ ). However, both anomalies in [CO] and  $\delta^{18}\text{O}(\text{CO})$  manifest clear but complex influences of the concomitant  $[\text{O}_3]$ . That is, the C1 *in situ* and WAS data very likely evidence artefacts pertaining to the  $\text{O}_3$ -driven effect of the same nature. Below we discuss and quantify these influences.

Deleted: an opposite case

Deleted: is

Deleted: functions

Deleted: ascertain

### 239 3 Discussion

[11] Three factors may lead to the (artefact) distributions seen for C1 *in situ* [CO] at LMS  $\text{O}_3$  mixing ratios, namely:

[12] (i) Strong (linear) natural mixing, such as enhanced stratosphere-troposphere exchange (STE), when a [CO] outside the statistically expected range results from the integration of air having dissimilar ratios of the tracers' mixing ratios, *viz.*  $[\text{O}_3]:[\text{CO}]$ . For example, mixing of two air parcels in a 16%:84% proportion (by moles of air) with typical  $[\text{O}_3]:[\text{CO}]$  of 700:24 (stratospheric) and 60:125 (tropospheric), respectively, yields an integrated composition with  $[\text{O}_3]:[\text{CO}]$  of 598:40 which indeed corresponds to C1 data (this case is exemplified by the mixing curve in Fig. 1). Nonetheless, occurrences of rather high stratospheric CO mixing ratios (in our case, 40 nmol/mol at the concomitant  $[\text{O}_3]$  of 500–600 nmol/mol compared to the typical 24–26 nmol/mol) are rare. For instance, a deep STE similar to that described by Pan *et al.* (2004) was observed by C2 only once (*cf.* the outliers at  $[\text{O}_3]$  of 500 nmol/mol in Fig. 1), whereas the C1 outliers were exclusively registered in some 12 flights during

Deleted: such as

Deleted: the

Deleted: abundances

Deleted: abundances

Deleted: 5

Deleted: 5

Deleted: ~

Deleted: 0

Deleted: (compared to the typical 24–26 nmol/mol)

Deleted: ~

268 1997–2001. No relation between these outliers and the large-scale [CO] perturbation due to ex-  
269 tensive biomass burning in 1997/1998 (Novelli *et al.*, 2003) is established, otherwise elevated  
270 CO mixing ratios should manifest themselves at lower [O<sub>3</sub>] as well. Other tracers detected in  
271 CARIBIC provide supporting evidence against such strongly STE-mixed air having been captured  
272 by C1. That is, the binned distributions for water vapour and de-trended N<sub>2</sub>O mixing ratios  
273 (not shown here) are similar for C1 and C2. Whereas the small relative variations in atmospheric  
274 [N<sub>2</sub>O] merely confirm matching [O<sub>3</sub>] distributions in CARIBIC, the stratospheric [H<sub>2</sub>O]  
275 distributions witness no [O<sub>3</sub>]:[H<sub>2</sub>O] values corresponding to those of the C1 outliers, suggesting  
276 the latter being unnaturally low.

277 [13] (ii) Mixing effects can also occur artificially, originating from sampling peculiarities or data  
278 processing. Since the CARIBIC platform is not stationary, about 5 s long sampling of an *in situ*  
279 air probe in C1 implies integration of the air compositions encountered along some hundred metres,  
280 owing to the high aircraft speed. This distance may cover a transect between tropospheric  
281 and stratospheric filaments of different compositions. The effect of such ‘translational mixing’  
282 can be simulated by averaging the sampling data with higher temporal frequency over longer  
283 time intervals. In this respect, the substantially more frequent CO data in C2 (sampling interval  
284 <1 s) were artificially averaged over a set of increasing intervals to reckon whether the long  
285 sampling period in C1 could be the culprit for skewing its CO–O<sub>3</sub> distribution. As a result, the  
286 original C2 data and their averages (equivalent to the C1 CO sample injection time) differ negligibly,  
287 as do the respective [O<sub>3</sub>]:[CO] values. Our simulations of the ‘translational mixing’ effects confirm that  
288 the actual C2 CO–O<sub>3</sub> distribution, in the region of interest ([O<sub>3</sub>] of  
289 540–620 nmol/mol) remains insensitive to averaging intervals, of up to 300 s. Furthermore, a  
290 very strong artificial mixing with an averaging interval of at least 1200 s (comparable to C1  
291 WAS sampling time) is required to yield the averages from the C2 data with [O<sub>3</sub>]:[CO] characteristic  
292 for the C1 outliers.

293 [14] (iii) In view of the above, it is unlikely that any natural or artificial mixing processes are involved  
294 in the stratospheric [CO] discrepancies seen in C1. We therefore conclude that the sample  
295 contamination in C1 occurred prior to the probed air reaching the analytical instrumentation  
296 and WAS sampling tanks in the container, since clearly elevated stratospheric CO mixing ratios  
297 are common to WAS and *in situ* data. Two more indications, *viz.* growing [CO] discrepancy  
298 with increasing O<sub>3</sub> abundance, and the strong concomitant signal in δ<sup>18</sup>O(CO), suggest that O<sub>3</sub>-  
299 mediated production of CO took place. Further, by confronting the C1 and C2 [CO] measure-

Deleted: the

Deleted: similar to that for [CO] vs. [O<sub>3</sub>] presented in Fig. 1,

Deleted: greatly

Deleted: in

Deleted: statistics

Deleted: CO

Deleted: much

Deleted: T

Deleted: statistic

Deleted: integration

Deleted: /sampling

Deleted: imply

Deleted: photochemical

314 ments in a regression analysis, (detailed in Appendix A), we quantify the artefact component  
 315  $[CO]_e$  being chiefly a function of  $O_3$  mixing ratio, as

$$[CO]_e = b \cdot [O_3]^2, \quad b = (5.19 \pm 0.12) \cdot 10^{-5} \text{ [mol/nmol]}, \quad (1)$$

316 which is equivalent to 8–18 nmol/mol throughout the respective  $[O_3]$  range of  
 317 400–620 nmol/mol (see Fig. 1 (d)). Subtracting this artefact signal yields the corrected *in situ*  
 318 C1 CO– $O_3$  distribution conforming to that of C2 (*cf.* red symbols in Fig. 1 (a)).

319 [15] Importantly, since we can quantify the contamination strength using only the  $O_3$  mixing ra-  
 320 tio, the continuous *in situ* C1  $[O_3]$  data allow estimating the integral artefact CO component in  
 321 each WAS sample and, if the isotope ratio of contaminating  $O_3$  is known, to derive the initial  
 322  $\delta^{18}O(CO)$ . The latter, as it was mentioned above, is subject to strong sample-mixing effects,  
 323 which is witnessed by  $\delta^{18}O(CO)$  outliers even at relatively high  $[CO]$  up to 100 nmol/mol. Ac-  
 324 counting for such cases is, however, problematic since it is necessary to distinguish the propor-  
 325 tions of the least modified (tropospheric) and significantly affected (stratospheric) components  
 326 in the resultant WAS sample mix. Since this information is not available, we applied an *ad hoc*  
 327 correction approach, as described in the following. This approach is capable of determining the  
 328 contamination source (*i.e.*,  $O_3$ ) isotope signature as well,

### 3.1 Contamination isotope signatures

329 [16] We use the differential mixing model (MM, originally known as the “Keeling-plot”), be-  
 330 cause it requires only the estimate of the artefact component mixing ratio, but no assumptions  
 331 on the (unknown) shares and isotope signatures of the air portions mixed in a given WAS tank.  
 332 The MM parameterises the admixing of the portion of artefact CO to the WAS sample with the  
 333 “true” initial composition, as formulated below:

$$[CO]_a = [CO]_t + [CO]_c \quad (2)$$

$${}^i\delta_a [CO]_a = {}^i\delta_t [CO]_t + {}^i\delta_c [CO]_c \quad (3)$$

334 where indices  $a$ ,  $c$  and  $t$  distinguish the mixing ratios and isotope compositions  ${}^i\delta$  ( $^{18}O$  and  $^{13}C$ )  
 335 for  $^{13}C$  and  $^{18}O$ , respectively) pertaining to the analysed sample, estimated contamination and  
 336 “true” composition sought (*i.e.*,  $[CO]_t$  and  ${}^i\delta_t$ ), respectively. Here the contamination strength  
 337  $[CO]_c$  is derived by integrating Eq. (1) using the *in situ* C1  $[O_3]$  data for each WAS sample. By  
 338 rewriting the above equation with respect to the isotope signature of the analysed CO, one obtains:

$${}^i\delta_a = {}^i\delta_c + ({}^i\delta_t - {}^i\delta_c) [CO]_t / [CO]_a \quad (4)$$

Deleted: kinetic framework

Deleted: CO

Deleted: abundance

Deleted: abundance

Deleted: s

Deleted: In reality, however,

Deleted: therefore

Deleted: (which

Deleted: ), as described in the following

Deleted: Practically we resort to

Deleted:  $\begin{cases} \delta_a C_a = C_t \delta_t + C_c \delta_c \\ C_a \equiv C_t + C_c \end{cases}$

Deleted:  $\begin{cases} \delta_a C_a = C_t \delta_t + C_c \delta_c \\ C_a \equiv C_t + C_c \end{cases}$

Deleted: abundances C

Deleted: (

Deleted: )

Deleted:  $\delta_a = \delta_c + (\delta_t - \delta_c) C_t / C_a$

Deleted: 3

354 which signifies that linear regression of  ${}^i\delta_a$  as a function of the reciprocal of  $[\text{CO}]_a$  yields the es-  
355 timated contamination signature  ${}^i\delta_c$  at  $([\text{CO}]_a)^{-1} \rightarrow 0$  when invariable "true" compositions  
356  $([\text{CO}]_t, {}^i\delta_t)$  are taken (the Keeling plot detailing these calculations is shown in Fig. 5). We there-  
357 fore apply the MM described by Eq. (2) to the subsets of samples picked according to the same  
358 reckoned  $[\text{CO}]_a$  (within a  $\pm 2$  nmol/mol window,  $n > 7$ ). Such selection, however, may be insuf-  
359 ficient: Due to the strong sampling effects in the WAS samples (see previous Section), it is possi-  
360 ble to encounter samples that integrate different air masses to the same  $[\text{CO}]_a$  but rather differ-  
361 ent average  ${}^i\delta_t$ . The solution in this case is to refer to the goodness of the MM regression fit, be-  
362 cause the  $R^2$  intrinsically measures the linearity of the regressed data, *i.e.* closeness of the "true"  
363 values in a regarded subset of samples, irrespective of underlying reasons for that.

364 [17] Higher  $R^2$  values thus imply higher consistency of the estimate, as demonstrated in Fig. 6  
365 showing the calculated  ${}^i\delta_c$  for  $[\text{CO}]_a$  below 80 nmol/mol as a function of the regression  $R^2$ . The  
366 latter decreases with greater  $[\text{CO}]_a$  (*i.e.*, larger sample subset size, since tropospheric air is more  
367 often encountered) and, correspondingly, larger variations in  ${}^i\delta_t$ . Ultimately, at lower  $R^2$  the in-  
368 ferred  ${}^{18}\delta_c$  converge to values slightly above zero expected for uncorrelated data, *i.e.* C1  
369  $\delta^{18}\text{O}(\text{CO})$  tropospheric average. A similar relationship is seen for the  ${}^{13}\delta_c$  values (they converge  
370 around  $-28\text{‰}$ ), however, there are no consistent estimates found ( $R^2$  is generally below 0.4).  
371 Since such is not the case for  $\delta^{18}\text{O}$ , the MM is not sufficiently sensitive to the changes caused  
372 by the contamination, which implies that the artefact CO  $\delta^{13}\text{C}$  should be within the range of the  
373 "true"  $\delta^{13}\text{C}(\text{CO})$  values. Interestingly, the MM is rather responsive to the growing fraction of  
374 the  $\text{CH}_4$ -derived component in CO with increasing  $[\text{O}_3]$ , as the  ${}^{13}\delta_c$  value of  $-(47.2 \pm 5.8)\text{‰}$  in-  
375 ferred at  $R^2$  above 0.4 is characteristic for the  $\delta^{13}\text{C}$  of methane in the UT/LMS. It is important to  
376 note that we have accounted for the biases in the analysed C1 WAS  $\delta^{13}\text{C}(\text{CO})$  expected from  
377 the mass-independent isotope composition of  $\text{O}_3$  (see details in Appendix B).

378 [18] We derive the "best-guess" estimate of the admixed CO  ${}^{18}\text{O}$  signature at  ${}^{18}\delta_c =$   
379  $+(92.0 \pm 8.3)\text{‰}$ , which agrees with the other MM results obtained at  $R^2$  above 0.75. Taking the  
380 same subsets of samples, the concomitant  ${}^{13}\text{C}$  signature matches  ${}^{13}\delta_c = -(23.3 \pm 8.6)\text{‰}$ , indeed at  
381 the upper end of the expected LMS  $\delta^{13}\text{C}(\text{CO})$  variations of  $-(25-31)\text{‰}$ . Because of that, the  
382 MM is likely insensitive to the changes in  $\delta^{13}\text{C}(\text{CO})$  caused by the contamination (the corre-  
383 sponding  $R^2$  values are below 0.1). Upon the correction using the inferred  ${}^{18}\delta_c$  value, the C1  
384 WAS  $\delta^{18}\text{O}(\text{CO})$  data agree with B96 (shown with red symbols in Fig. 3). That is, variations in  
385 the observed  $\text{C}^{18}\text{O}$  are driven by (i) the seasonal/regional changes in the composition of tropo-  
386 spheric air and by (ii) the degree of mixing or replacement of the latter with the stratospheric

Deleted:  ${}^i$

Deleted:  $C_i$

Deleted:  $C_i$

Deleted:  $C_i$

Deleted: nformably

Deleted:  ${}^{18}\text{O}$  signatures

Deleted:  ${}^{13}\text{C}$

Deleted: signatures

Deleted: -

Deleted: -

Deleted: appear adequate

Deleted: Fig. 2

399 component that is less variable in  $^{18}\text{O}$ . This is seen as stretching of the scattered tropospheric  
400 values ([CO] above 60 nmol/mol) towards  $\delta^{18}\text{O}(\text{CO})$  of around  $-10\text{‰}$  at [CO] of 25 nmol/mol,  
401 respectively. The corrected C1  $\delta^{13}\text{C}(\text{CO})$  data (shown in Fig. 7) are found to be in a  $\pm 1\text{‰}$   
402 agreement with the observations by B96, except for several deep stratospheric samples ([CO]  
403 below 40 nmol/mol). The latter were encountered during “ozone hole” conditions and carried  
404 extremely low  $\delta^{13}\text{C}(\text{CO})$  values, which was attributed to the reaction of methane with available  
405 free Cl radicals (Brenninkmeijer *et al.*, 1996).

Deleted: in a mixing fashion

Deleted: ~

Deleted: "

Deleted: "

Deleted: abundances

### 3.2 Estimate of $\delta^{18}\text{O}(\text{O}_3)$

406 [19] The contamination  $^{18}\text{O}$  signature inferred here ( $^{18}\delta_c = +(92.0 \pm 8.3)\text{‰}$ ) likely pertains to  $\text{O}_3$   
407 and is comparable to  $\delta^{18}\text{O}(\text{O}_3)$  values measured in the stratosphere at temperatures about 30 K  
408 lower than those encountered in the UT/LMS by C1 (see Table 1 for comparison). If no other  
409 factors are involved (see below), this discrepancy in  $\delta^{18}\text{O}(\text{O}_3)$  should be attributed to the local  
410 conditions, *i.e.* the higher pressures (typically 240–270 hPa for C1 cruising altitudes) at which  
411  $\text{O}_3$  was formed. Indeed, the molecular lifetime (the period through which the species’ isotope  
412 reservoir becomes entirely renewed, as opposed to the “bulk” lifetime) of  $\text{O}_3$  encountered along  
413 the C1 flight routes is estimated on the order of minutes to hours at daylight (H. Riede, Max  
414 Planck Institute for Chemistry, 2010), thus the isotope composition of the photochemically re-  
415 generated  $\text{O}_3$  resets quickly according to the local conditions. Virtual absence of sinks, in turn,  
416 leads to “freezing” of the  $\delta^{18}\text{O}(\text{O}_3)$  value during night in the UT/LMS. Verifying the current  
417  $\delta^{18}\text{O}(\text{O}_3)$  estimate against the kinetic data, in contrast to the stratospheric cases, is problematic.  
418 The laboratory studies on  $\text{O}_3$  formation to date have scrutinised the concomitant kinetic isotope  
419 effects (KIEs) as a function of temperature at only low pressures (67 mbar); the attenuation of  
420 the KIEs with increasing pressure was studied only at room temperatures (see Table 1, also  
421 Brenninkmeijer *et al.* (2003) for references). A rather crude attempt may be undertaken by as-  
422 suming that the formation KIEs become attenuated at higher pressures in a similar (proportion-  
423 al) fashion to that measured at 320 K, however applied to the nominal low-pressure values  
424 reckoned at (220–230) K. A decrease in  $\delta^{18}\text{O}(\text{O}_3)$  of about (6–8)‰ is expected from such cal-  
425 culation (*cf. last row in Table 1*), yet accounting for a mere one-half of the (13–15)‰ discrep-  
426 ancy between the stratospheric  $\delta^{18}\text{O}(\text{O}_3)$  values and  $^{18}\delta_c$ .

Deleted: unambiguous

Deleted: '

Deleted: 50 Torr

Deleted: 5.9

Deleted: 7.6

Deleted: .3

Deleted: 4.6

427 [20] Lower  $^{18}\delta_c$  values could result from possible isotope fractionation accompanying the pro-  
428 duction of the artefact CO. Although not quantifiable here, oxygen KIEs in the  $\text{O}_3 \rightarrow \text{CO}$  con-  
429 version chain cannot be ruled out, recalling that the intermediate reaction steps are not identifi-

442 able and the artefact CO represents at most 4% of all O<sub>3</sub> molecules. Furthermore, the yield  $\lambda_{O_3}$   
443 of CO from O<sub>3</sub> may be lower than unity (see details in Appendix A). On the other hand, the in-  
444 ference that the contamination strength primarily depends on [O<sub>3</sub>] indicates that the kinetic frac-  
445 tionation may have greater effect on the carbon isotope ratios of the artefact CO produced (the  
446  $^{13}\delta_c$  values) in contrast to the oxygen ones. That is because all reactive oxygen available from  
447 O<sub>3</sub> becomes converted to CO, whilst the concomitant carbon atoms are drawn from a virtually  
448 unlimited pool whose apparent isotope composition is altered by the magnitude of the  $^{13}\text{C}$  KIEs.

449 [21] Besides KIEs, selectivity in the transfer of O atoms from O<sub>3</sub> to CO affects the resulting  $^{18}\delta_c$   
450 value. The terminal O atoms in O<sub>3</sub> are enriched with respect to the molecular (bulk) O<sub>3</sub> compo-  
451 sition when the latter is above  $+70\text{‰}$  in  $\delta^{18}\text{O}$  (Janssen, 2005; Bhattacharya *et al.*, 2008), there-  
452 fore an incorporation of only central O atoms into the artefact CO molecules should result in a  
453 reduced apparent  $^{18}\delta_c$  value. Such exclusive selection is, however, less likely from the kinetic  
454 standpoint and was not observed in available laboratory studies (see Savarino *et al.* (2008) for a  
455 review). For instance, Röckmann *et al.* (1998a) established the evidence of direct O transfer  
456 from O<sub>3</sub> to the CO produced in alkene ozonolysis. A reanalysis of their results (in light of find-  
457 ings of Bhattacharya *et al.* (2008)) suggests that usually the terminal atoms of the O<sub>3</sub> molecule  
458 become transferred (their ratio over the central ones changes from the bulk 2:1 to 1:0 for vari-  
459 ous species). Considering the alternatives of the O transfer in our case (listed additionally in  
460 Table 1), the equiprobable incorporation of the terminal and central O<sub>3</sub> atoms into CO should  
461 result in the  $\delta^{18}\text{O}(\text{O}_3)$  value in agreement with the “crude” estimate based on laboratory data  
462 given above.

463 [22] Furthermore, the conditions that supported the reaction of O<sub>3</sub> (or its derivatives) followed by  
464 the production of CO are vague. A few hypotheses ought to be scrutinised here. First, a fast  
465 O<sub>3</sub> → CO conversion must have occurred, owing to short (*i.e.*, fraction of a second) exposure  
466 time of the probed air to the contamination. Accounting for the typical C1 air sampling condi-  
467 tions (these are: sampled air pressure of 240–270 hPa and temperature of 220–235 K outboard  
468 to 275–300 K inboard, sampling rate of  $12.85 \cdot 10^{-3} \text{ mol s}^{-1}$  corresponding to 350 L STP sam-  
469 pled in 1200 s, inlet/tubing volume gauged to yield exposure times of 0.01 to 0.1 s due to varia-  
470 ble air intake rate, [O<sub>3</sub>] of 600 nmol/mol), the overall reaction rate coefficient ( $k_c$  in Eq. (A3),  
471 from Appendix A) must be on the order of  $(6 \cdot 10^{-15} / \tau_c) \text{ molec}^{-1} \text{ cm}^3 \text{ s}^{-1}$ , where  $\tau_c$  is the exposure  
472 time. Assuming the case of a gas-phase CO production from a recombining O<sub>3</sub> derivative and  
473 an unknown carbonaceous compound X, the reaction rate coefficient for the latter ( $k_x$  in Eq. (A2),  
474 in Appendix A) must be unrealistically high, at least  $6 \cdot 10^{-10} \text{ molec}^{-1} \text{ cm}^3 \text{ s}^{-1}$  over  $\tau_c = 1/100 \text{ s}$ .

Deleted: ~

Deleted: ~

Deleted: ~

Deleted: ~

Deleted: es

Field Code Changed

Deleted: (A1)

Deleted: s<sup>-1</sup>

Deleted: x

Deleted: r

Field Code Changed

Deleted: (A1)

Deleted: ~



486 This number decreases proportionally with growing  $\tau_c$  and  $[X]$ , if we take less strict exposure  
487 conditions. Nonetheless, in order to provide the amounts of artefact CO we detect, a minimum  
488 mixing ratio of 20 nmol/mol (or up to 4  $\mu\text{g}$  of C per flight) of X is required, which is not availa-  
489 ble in the UT/LMS from the species readily undergoing ozonolysis, *e.g.* alkenes.

Deleted: abundance

490 [23] Second, a more complex heterogeneous chemistry on the inner surface of the inlet or sup-  
491 plying tubing may be involved. Such can be the tracers' surface adsorption, (catalytic) decom-  
492 position of  $\text{O}_3$  and its reaction with organics or with surface carbon that also may lead to the  
493 production of CO (Oyama, 2000). Evidence exists for the dissociative adsorption of  $\text{O}_3$  on the  
494 surfaces with subsequent production of the reactive atomic oxygen species (see, *e.g.*,  
495 Li *et al.*, 1998, also Oyama, 2000). It is probable that sufficient amounts of organics have re-  
496 mained on the walls of the sampling line exposed to highly polluted tropospheric air, to be later  
497 broken down by the products of the heterogeneous decomposition of the ample stratospheric  $\text{O}_3$ .  
498 Unfortunately, the scope for a detailed quantification of intricate surface effects in the C1 CO  
499 contamination problem is very limited.

## 500 4 Conclusions

501 [24] Recapitulating, the *in situ* measurements of CO and  $\text{O}_3$  allowed us to unambiguously quanti-  
502 fy the artefact CO production from  $\text{O}_3$  likely in the sample line of the CARIBIC-1 instrumenta-  
503 tion. Strong evidence to that is provided by the isotope CO measurements. We demonstrate the  
504 ability of the simple mixing model ("Keeling-plot" approach) to single out the contamination  
505 isotope signatures even in the case of a large sampling-induced mixing of the air with very dif-  
506 ferent compositions. Obtained as a collateral result, the estimate of the  $\delta^{18}\text{O}(\text{O}_3)$  in the UT/LMS  
507 appears adequate, calling, however, for additional laboratory data (*e.g.*, the temperature-driven  
508 variations of the  $\text{O}_3$  formation KIE at pressures above 100 hPa) for a more unambiguous verifi-  
509 cation.

## 510 Appendix A. Contamination assessment

Deleted: kinetic framework

511 We quantify the C1 CO contamination strength (denoted  $[\text{CO}]_c$ , obtained by discriminating the  
512 C1 outliers from respective C2 data) in a sequence of regression analyses. We foremost ascer-  
513 tain that no other species or operational parameter (*e.g.* temperature, pressure, flight duration,  
514 season, latitude, time of day, *etc.*) measured in C1 appear to determine (*e.g.*, systematically cor-  
515 relate with)  $[\text{CO}]_c$ , except that for  $[\text{O}_3]$ . We hypothesise therefore that a production of artefact

Deleted: We infer the functional dependence of

CO molecules was initiated by O<sub>3</sub> (via either its decomposition or a reaction with an unknown educt) and proceeded with incorporation of carbon (donated by some carbonaceous species X) and oxygen (donated by O<sub>3</sub> or its derivatives) atoms into final CO. Despite that neither the actual reaction chain nor its intermediates are known, it is possible to describe the artefact CO component produced (hereinafter curly brackets {} denote number densities) as

$$\{CO\}_c = \lambda_{O_3} \nu \tau_c \quad (A1)$$

where the yield  $\lambda_{O_3}$ , a diagnostic quantity, relates the amount of artefact CO molecules produced to the total number of O<sub>3</sub> molecules consumed in the system,  $\tau_c$  denotes the reaction time (period throughout which sampled air is exposed to contamination), and  $\nu$  stands for the overall rate of the reaction chain. The latter, being regarded macroscopically (empirically), is parameterised to account for the order of reaction chain rate with respect to hypothesised reactants (McNaught and Wilkinson, 1997) as

$$\nu = k \{X\}^K \{O_3\}^\kappa \quad (A2)$$

where  $\kappa$  and  $K$  are the partial orders with respect to X and O<sub>3</sub> number densities, respectively, and  $k$  is the rate coefficient. Here it is implied that changes to  $\{X\}$  and  $\{O_3\}$  are negligible throughout the exposure time  $\tau_c$  (typically < 0.1 s for C1 sample line). As stated above, we find that variations in  $\{CO\}_c$  correlate exclusively with variations in  $\{O_3\}$ , hence Eq. (A2) can be reduced by assuming constancy of  $\{X\}$  and  $K$  to:

$$\nu_c = k_c \{O_3\}^\kappa \quad (A3)$$

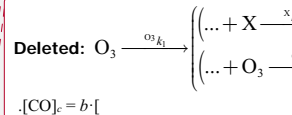
Here,  $k_c = k\{X\}^K$  (often referred to as pseudo-first-order or “observed” rate coefficient) quantifies the rate of reaction chain exclusively propelled by O<sub>3</sub>. Finally, using Eqs. (A1) and (A3), the artefact  $\{CO\}_c$  component is expressed as

$$\{CO\}_c = b \cdot \{O_3\}^\kappa, \quad b = \lambda_{O_3} k_c \tau_c \quad (A4)$$

where the constant proportionality factor  $b$  integrates the influence of the unknown (and as we explicate below, likely invariable)  $\{X\}$ ,  $k$ ,  $K$  and  $\tau_c$ .

Eq. (A4) defines the regression expression using which we attempt to fit the values of  $\{CO\}_c$  as a function of  $\kappa$ ,  $\{O_3\}$  and  $b$ . In the first regression iteration we keep both  $\kappa$  and  $b$  as free parameters, which provides best approximation at  $\kappa = 2.06 \pm 0.38$ , suggesting reactions of two O<sub>3</sub> molecules in case elementary reactions constitute the reaction mechanism, or two elementary steps involving O<sub>3</sub> or its derivatives in case a stepwise reaction is involved (McNaught and Wilkinson, 1997). In a subsequent regression iteration we set  $\kappa = 2$ , which yields better (as opposed to the first iteration) estimate of  $b$  of  $(5.19 \pm 0.12) \cdot 10^{-5}$  mol/nmol ( $\pm 1\sigma$ ,

Deleted: s:



Deleted: ]

Deleted: 1

Deleted: Eq. (A1) reads that production of an artefact CO molecules is initiated by O<sub>3</sub> (via either its decomposition or a reaction with an unknown educt) and is followed by a set of unknown reactions which proceed via unknown educts or products (denoted with ellipses), however requiring at some step an incorporation of carbon (donated by carbonaceous species X) and oxygen (also possible in secondary O<sub>3</sub> reactions) atoms into final CO. C

Deleted: <#>s  $K$  and  $\kappa$  describes the stoichiometry of the system with respect to ozone, i.e. how many (rate-determining) reactions of X and O<sub>3</sub> ((with the individual unknown rate coefficients  $x_k$  and  $o_3 k_i$  or its derivatives)) may have lead to production of one artefact CO, respectively. The yield  $\lambda_{O_3}$ , a diagnostic quantity, relates the amount of artefact CO molecules produced to the total number of O<sub>3</sub> molecules consumed in the system. Based on Eq. (A1), the functional dependence of the artefact CO component is expressed as

Deleted: (A2)

Deleted: ed

Deleted: [

Deleted: ]

Deleted: [

Deleted: ]

Deleted: ,  $K$  and  $[X]$  (the latter was chosen iteratively from a set of candidates ... [2])

Deleted: Finally, regressing  $C_c$  using Eq. (A3)

Deleted: its

Deleted: as a function of [O<sub>3</sub>]

Deleted: chain

Deleted: At

Deleted: the product ( $\lambda_{O_3} k_c \tau_c$ ) that proportionates the CO contamination ... [3]

635 adj.  $R^2 = 0.83$ , red.  $\chi^2 = 4.0$ ; here the equivalent value in mole fraction units is quoted for the  
636 convenience of relating fitted  $[\text{CO}]_c$  and  $[\text{O}_3]_c^2$ . At last, we ascertain that the best regression re-  
637 sults are obtained particularly at  $\kappa = 2$ , as indicated by the regression statistic ( $R^2$  and  $\chi^2$ ) that  
638 asymptotically improves when a set of regressions with neighbouring (*i.e.* below and above 2)  
639 integer values of  $\kappa$  is compared. The low uncertainty (within  $\pm 3\%$ ) associated with the estimate  
640 of  $b$  confirms an exclusive dependence of the contamination source on the  $\text{O}_3$  mixing ratio, as  
641 well as much similar reaction times  $\tau_c$ . The regressed value of  $[\text{CO}]_c$  as a function of  $[\text{O}_3]$  is pre-  
642 sented in Fig. 1 (d) (solid line). It is possible to constrain the overall yield  $\lambda_{\text{O}_3}$  of CO molecules  
643 in the artefact source chain to be between 0.5 and 1, comparing the magnitude of  $[\text{CO}]_c$  to the  
644 discrepancy between the  $[\text{O}_3]$  measured in C1 and C2 ( $\pm 20$  nmol/mol, taken equal to the  $[\text{O}_3]$   
645 bin size owing to the  $\text{N}_2\text{O}-\text{O}_3$  and  $\text{H}_2\text{O}-\text{O}_3$  distributions matching well between the datasets).  
646 Lower  $\lambda_{\text{O}_3}$  values, otherwise, should have resulted in a noticeable (*i.e.*, greater than  
647 20 nmol/mol) decrease in the C1  $\text{O}_3$  mixing ratios, with respect to the C2 levels.

Deleted: are used here

Deleted: of

Deleted: is

Deleted: abundance

Deleted: abundances

## 648 Appendix B. Corrections to measured $\delta^{13}\text{C}(\text{CO})$ values due to the oxygen

### 649 MIF

650 [26] Atmospheric  $\text{O}_3$  carries an anomalous isotope composition (or mass-independent fractiona-  
651 tion, MIF) with a substantially higher relative enrichment in  $^{17}\text{O}$  over that in  $^{18}\text{O}$  (above  $+25\%$   
652 in  $\Delta^{17}\text{O} = (\delta^{17}\text{O}+1)/(\delta^{18}\text{O}+1)^\beta - 1$ ,  $\beta = 0.528$ ) when compared to the majority of terrestrial oxy-  
653 gen reservoirs that are mass-dependently fractionated (*i.e.*, with  $\Delta^{17}\text{O}$  of 0%) (see Brenninkmei-  
654 jer *et al.* (2003) and refs. therein). CO itself also has an unusual oxygen isotopic composition,  
655 possessing a moderate tropospheric MIF of around  $+5\%$  in  $\Delta^{17}\text{O}(\text{CO})$  induced by the sink KIEs  
656 in reaction of CO with OH (Röckmann *et al.*, 1998b; Röckmann *et al.*, 2002) and a minor  
657 source effect from the ozonolysis of alkenes (Röckmann *et al.*, 1998a; Gromov *et al.*, 2010). A  
658 substantial contamination of CO by  $\text{O}_3$  oxygen induces proportional changes to  $\Delta^{17}\text{O}(\text{CO})$  that  
659 largely exceed its natural atmospheric variation. On the other hand, the MIF has implications in  
660 the analytical determination of  $\delta^{13}\text{C}(\text{CO})$ , because the presence of  $\text{C}^{17}\text{O}$  species interferes with  
661 the mass-spectrometric measurement of the abundances of  $^{13}\text{CO}$  possessing the same basic mo-  
662 lecular mass ( $m/z$  is 45). When inferring the exact  $\text{C}^{17}\text{O}/\text{C}^{18}\text{O}$  ratio in the analysed sample is not  
663 possible, analytical techniques usually involve assumptions (*e.g.*, mass-dependently fractionated  
664 compositions or a certain non-zero  $\Delta^{17}\text{O}$  value) with respect to the  $\text{C}^{17}\text{O}$  abundances  
665 (Assonov and Brenninkmeijer, 2001). In effect for the C1 CO data, the artefact CO produced

Deleted: ~

672 from O<sub>3</sub> had contributed with unexpectedly high C<sup>17</sup>O abundances that led to the overestimated  
673 δ<sup>13</sup>C(CO) analysed. The respective bias <sup>13</sup>δ<sub>b</sub> is quantified using

$${}^{13}\delta_b = 7.26 \cdot 10^{-2} \Delta^{17}\text{O}(\text{CO}), \quad (\text{B1})$$

674 where the actual Δ<sup>17</sup>O(CO) value is approximated from the natural CO MIF signal <sup>17</sup>Δ<sub>n</sub> and the  
675 typical O<sub>3</sub> MIF composition <sup>17</sup>Δ<sub>c</sub> as

$$\Delta^{17}\text{O}(\text{CO}) = ({}^{17}\Delta_n [\text{CO}]_a - [\text{CO}]_c) + {}^{17}\Delta_c [\text{CO}]_c ([\text{CO}]_a)^{-1}. \quad (\text{B2})$$

676 Here  $[\text{CO}]_a$  and  $[\text{CO}]_c$  denote the analysed CO mixing ratio and contamination magnitude, re-  
677 spectively, used in the contamination assessment (see Appendix A, Eq. (A3)) and in calcula-  
678 tions with the MM (see Sect. 3.1). For the purpose of the current estimate it is sufficient to take  
679 <sup>17</sup>Δ<sub>n</sub> of +5‰ representing equilibrium enrichments expected in the remote free troposphere and  
680 UT/LMS. For the O<sub>3</sub> MIF signature <sup>17</sup>Δ<sub>c</sub>, the value of +30‰ (the average Δ<sup>17</sup>O(O<sub>3</sub>) expected  
681 from the kinetic laboratory data at conditions met along the C1 flight routes, see Sect. 3.2 and  
682 Table 1) is adopted. The coefficient that proportionates <sup>13</sup>δ<sub>b</sub> and Δ<sup>17</sup>O in Eq. (B1) is derived by  
683 linearly regressing the δ<sup>13</sup>C(CO) biases (simulated using the calculation apparatus detailed by  
684 Assonov and Brenninkmeijer, 2001) as a function of Δ<sup>17</sup>O(CO) varying within a (0–30)‰  
685 range for the CO with initially unaccounted MIF (*e.g.*, the sample is assumed to be mass-  
686 dependently fractionated). It therefore quantifies some extra +(0.726±0.003)‰ in the analysed  
687 δ<sup>13</sup>C(CO) per every +10‰ of Δ<sup>17</sup>O(CO) excess. The most contaminated C1 WAS CO samples  
688 at [O<sub>3</sub>] above 300 nmol/mol are estimated to bear Δ<sup>17</sup>O(CO) of (6–12)‰ corresponding to frac-  
689 tions of (0.10–0.27) of the artefact CO in the sample. Accordingly, the reckoned δ<sup>13</sup>C(CO) bi-  
690 ases span (0.5–0.9)‰. Although not large, these well exceed the δ<sup>13</sup>C(CO) measurement preci-  
691 sion of ±0.1‰ and were corrected for, and therefore are taken into account in the calculations  
692 with the MM presented in Sect. 3.1.

Deleted: abundance

Deleted: kinetic framework

## 693 Acknowledgements

694 [27] The authors are indebted to Claus Koepfel, Dieter Scharffe and Dr. Andreas Zahn for their  
695 work and expertise on the carbon monoxide and ozone measurements in C1 and C2. Hella  
696 Riede is acknowledged for comprehensive estimates of the species lifetimes along the  
697 CARIBIC flight routes. We are grateful to Dr. Taku Umezawa, Dr. Angela K. Baker, Dr. Em-  
698 ma C. Leedham, Dr. Sergey Assonov, the anonymous reviewer and Dr. Jan Kaiser for the help-  
699 ful discussions and comments on the manuscript.

## 702 References

- 703 Assonov, S. S. and Brenninkmeijer, C. A. M.: A new method to determine the  $^{17}\text{O}$  isotopic abundance in  
704  $\text{CO}_2$  using oxygen isotope exchange with a solid oxide, *Rapid Commun. Mass Spectrom.*, **15**,  
705 2426–2437, doi: [10.1002/rcm.529](https://doi.org/10.1002/rcm.529), 2001.
- 706 Assonov, S. S. and Brenninkmeijer, C. A. M.: A redetermination of absolute values for  $^{17}\text{R}_{\text{VPDB-CO}_2}$  and  
707  $^{17}\text{R}_{\text{VSMOW}}$ , *Rapid Commun. Mass Spectrom.*, **17**, 1017–1029, doi: [10.1002/Rcm.1011](https://doi.org/10.1002/Rcm.1011), 2003.
- 708 Assonov, S. S., Brenninkmeijer, C. A. M., Koepfel, C., and Röckmann, T.:  $\text{CO}_2$  isotope analyses using  
709 large air samples collected on intercontinental flights by the CARIBIC Boeing 767,  
710 *Rapid Commun. Mass Spectrom.*, **23**, 822–830, doi: [10.1002/rcm.3946](https://doi.org/10.1002/rcm.3946), 2009.
- 711 Bhattacharya, S. K., Pandey, A., and Savarino, J.: Determination of intramolecular isotope distribution of  
712 ozone by oxidation reaction with silver metal, *J. Geophys. Res. Atm.*, **113**, D03303,  
713 doi: [10.1029/2006jd008309](https://doi.org/10.1029/2006jd008309), 2008.
- 714 Brenninkmeijer, C. A. M.: Measurement of the abundance of  $^{14}\text{CO}$  in the atmosphere and the  $^{13}\text{C}/^{12}\text{C}$  and  
715  $^{18}\text{O}/^{16}\text{O}$  ratio of atmospheric CO with applications in New Zealand and  
716 Antarctica, *J. Geophys. Res. Atm.*, **98**, 10595–10614, doi: [10.1029/93JD00587](https://doi.org/10.1029/93JD00587), 1993.
- 717 Brenninkmeijer, C. A. M., Müller, R., Crutzen, P. J., Lowe, D. C., Manning, M. R., Sparks, R. J., and van  
718 Velthoven, P. F. J.: A large  $^{13}\text{CO}$  deficit in the lower Antarctic stratosphere due to “Ozone Hole”  
719 Chemistry: Part I, Observations, *Geophys. Res. Lett.*, **23**, 2125–2128, doi: [10.1029/96gl01471](https://doi.org/10.1029/96gl01471), 1996.
- 720 Brenninkmeijer, C. A. M. and Röckmann, T.: Principal factors determining the  $^{18}\text{O}/^{16}\text{O}$  ratio of  
721 atmospheric CO as derived from observations in the southern hemispheric troposphere and lowermost  
722 stratosphere, *J. Geophys. Res. Atm.*, **102**, 25477–25485, doi: [10.1029/97JD02291](https://doi.org/10.1029/97JD02291), 1997.
- 723 Brenninkmeijer, C. A. M., Crutzen, P. J., Fischer, H., Gusten, H., Hans, W., Heinrich, G.,  
724 Heintzenberg, J., Hermann, M., Immelman, T., Kersting, D., Maiss, M., Nolle, M., Pitscheider, A.,  
725 Pohlkamp, H., Scharffe, D., Specht, K., and Wiedensohler, A.: CARIBIC – Civil aircraft for global  
726 measurement of trace gases and aerosols in the tropopause region, *J. Atmos. Oceanic Technol.*, **16**,  
727 1373–1383, doi: [10.1175/1520-0426\(1999\)016<1373:Ccafgm>2.0.Co;2](https://doi.org/10.1175/1520-0426(1999)016<1373:Ccafgm>2.0.Co;2), 1999.
- 728 Brenninkmeijer, C. A. M., Koepfel, C., Röckmann, T., Scharffe, D. S., Bräunlich, M., and Gros, V.:  
729 Absolute measurement of the abundance of atmospheric carbon monoxide, *J. Geophys. Res. Atm.*, **106**,  
730 10003–10010, doi: [10.1029/2000jd900342](https://doi.org/10.1029/2000jd900342), 2001.
- 731 Brenninkmeijer, C. A. M., Janssen, C., Kaiser, J., Röckmann, T., Rhee, T. S., and Assonov, S. S.: Isotope  
732 effects in the chemistry of atmospheric trace compounds, *Chem. Rev.*, **103**, 5125–5161,  
733 doi: [10.1021/Cr020644k](https://doi.org/10.1021/Cr020644k), 2003.
- 734 Brenninkmeijer, C. A. M., Crutzen, P., Boumard, F., Dauer, T., Dix, B., Ebinghaus, R., Filippi, D.,  
735 Fischer, H., Franke, H., Frieß, U., Heintzenberg, J., Helleis, F., Hermann, M., Kock, H. H.,  
736 Koepfel, C., Lelieveld, J., Leuenberger, M., Martinsson, B. G., Miemczyk, S., Moret, H. P.,  
737 Nguyen, H. N., Nyfeler, P., Oram, D., O'Sullivan, D., Penkett, S., Platt, U., Pucek, M., Ramonet, M.,  
738 Randa, B., Reichelt, M., Rhee, T. S., Rohwer, J., Rosenfeld, K., Scharffe, D., Schlager, H.,  
739 Schumann, U., Slemr, F., Sprung, D., Stock, P., Thaler, R., Valentino, F., van Velthoven, P.,  
740 Waibel, A., Wandel, A., Waschitschek, K., Wiedensohler, A., Xueref-Remy, I., Zahn, A.,  
741 Zech, U., and Ziereis, H.: Civil Aircraft for the regular investigation of the atmosphere based on an  
742 instrumented container: The new CARIBIC system, *Atmos. Chem. Phys.*, **7**, 4953–4976,  
743 doi: [10.5194/acp-7-4953-2007](https://doi.org/10.5194/acp-7-4953-2007), 2007.

744 Coplen, T. B.: Reporting of stable hydrogen, carbon, and oxygen isotopic abundances (Technical Report),  
745 *Pure Appl. Chem.*, **66**, 273–276, doi: [10.1351/pac199466020273](https://doi.org/10.1351/pac199466020273), 1994.

746 Craig, H.: Isotopic standards for carbon and oxygen and correction factors for mass-spectrometric analysis  
747 of carbon dioxide, *Geochim. Cosmochim. Acta*, **12**, 133–149, doi: [10.1016/0016-7037\(57\)90024-8](https://doi.org/10.1016/0016-7037(57)90024-8),  
748 1957.

749 Gonfiantini, R.: Standards for Stable Isotope Measurements in Natural Compounds, *Nature*, **271**,  
750 534–536, 1978.

751 Gromov, S., Jöckel, P., Sander, R., and Brenninkmeijer, C. A. M.: A kinetic chemistry tagging technique  
752 and its application to modelling the stable isotopic composition of atmospheric trace gases,  
753 *Geosci. Model Dev.*, **3**, 337–364, doi: [10.5194/gmd-3-337-2010](https://doi.org/10.5194/gmd-3-337-2010), 2010.

754 Guenther, J., Erbacher, B., Krankowsky, D., and Mauersberger, K.: Pressure dependence of two relative  
755 ozone formation rate coefficients, *Chem. Phys. Lett.*, **306**, 209–213,  
756 doi: [10.1016/S0009-2614\(99\)00469-8](https://doi.org/10.1016/S0009-2614(99)00469-8), 1999.

757 Janssen, C., Guenther, J., Krankowsky, D., and Mauersberger, K.: Temperature dependence of ozone rate  
758 coefficients and isotopologue fractionation in  $^{16}\text{O}$ – $^{18}\text{O}$  oxygen mixtures, *Chem. Phys. Lett.*, **367**,  
759 34–38, doi: [10.1016/S0009-2614\(02\)01665-2](https://doi.org/10.1016/S0009-2614(02)01665-2), 2003.

760 Janssen, C.: Intramolecular isotope distribution in heavy ozone ( $^{16}\text{O}^{18}\text{O}^{16}\text{O}$  and  $^{16}\text{O}^{16}\text{O}^{18}\text{O}$ ),  
761 *J. Geophys. Res. Atm.*, **110**, D08308, doi: [10.1029/2004jd005479](https://doi.org/10.1029/2004jd005479), 2005.

762 Johnston, J. C. and Thiemens, M. H.: The isotopic composition of tropospheric ozone in three  
763 environments, *J. Geophys. Res. Atm.*, **102**, 25395–25404, doi: [10.1029/97jd02075](https://doi.org/10.1029/97jd02075), 1997.

764 Krankowsky, D., Bartecki, F., Klees, G. G., Mauersberger, K., Schellenbach, K., and Stehr, J.:  
765 Measurement of heavy isotope enrichment in tropospheric ozone, *Geophys. Res. Lett.*, **22**, 1713–1716,  
766 doi: [10.1029/95gl01436](https://doi.org/10.1029/95gl01436), 1995.

767 Krankowsky, D., Lämmerzahl, P., Mauersberger, K., Janssen, C., Tuzson, B., and Röckmann, T.:  
768 Stratospheric ozone isotope fractionations derived from collected samples, *J. Geophys. Res. Atm.*, **112**,  
769 D08301, doi: [10.1029/2006jd007855](https://doi.org/10.1029/2006jd007855), 2007.

770 Li, W., Gibbs, G. V., and Oyama, S. T.: Mechanism of Ozone Decomposition on a Manganese Oxide  
771 Catalyst. 1. In Situ Raman Spectroscopy and Ab Initio Molecular Orbital  
772 Calculations, *J. Am. Chem. Soc.*, **120**, 9041–9046, doi: [10.1021/ja981441+](https://doi.org/10.1021/ja981441+), 1998.

773 Mauersberger, K.: Measurement of Heavy Ozone in the Stratosphere, *Geophys. Res. Lett.*, **8**, 935–937,  
774 doi: [10.1029/G1008i008p00935](https://doi.org/10.1029/G1008i008p00935), 1981.

775 McNaught, A. D. and Wilkinson, A.: IUPAC. Compendium of Chemical Terminology (the "Gold Book"),  
776 XML on-line corrected version: <http://goldbook.iupac.org> (2006-) created by  
777 M. Nic, J. Jirat, B. Kosata; updates compiled by A. Jenkins, doi: [10.1351/goldbook.O04322](https://doi.org/10.1351/goldbook.O04322), 1997.

778 Natrella, M.: NIST/SEMATECH e-Handbook of Statistical Methods., edited by: Croarkin, C. and  
779 Tobias, P., NIST/SEMATECH, <http://www.itl.nist.gov/div898/handbook/> (last access: 07 May 2014),  
780 2003.

781 Novelli, P. C., Masarie, K. A., and Lang, P. M.: Distributions and recent changes of carbon monoxide in  
782 the lower troposphere, *J. Geophys. Res.*, **103**, 19015–19033, doi: [10.1029/98jd01366](https://doi.org/10.1029/98jd01366), 1998.

783 Novelli, P. C., Masarie, K. A., Lang, P. M., Hall, B. D., Myers, R. C., and Elkins, J. W.: Reanalysis of  
784 tropospheric CO trends: Effects of the 1997–1998 wildfires, *J. Geophys. Res.*, **108**, 4464,  
785 doi: [10.1029/2002jd003031](https://doi.org/10.1029/2002jd003031), 2003.

- 786 Oyama, S. T.: Chemical and Catalytic Properties of Ozone, *Catal. Rev. Sci. Eng.*, **42**, 279–322,  
787 doi: [10.1081/cr-100100263](https://doi.org/10.1081/cr-100100263), 2000.
- 788 Pan, L. L., Randel, W. J., Gary, B. L., Mahoney, M. J., and Hints, E. J.: Definitions and sharpness of the  
789 extratropical tropopause: A trace gas perspective, *J. Geophys. Res. Atm.*, **109**, D23103,  
790 doi: [10.1029/2004jd004982](https://doi.org/10.1029/2004jd004982), 2004.
- 791 Röckmann, T., Brenninkmeijer, C. A. M., Neeb, P., and Crutzen, P. J.: Ozonolysis of nonmethane  
792 hydrocarbons as a source of the observed mass independent oxygen isotope enrichment in tropospheric  
793 CO, *J. Geophys. Res. Atm.*, **103**, 1463–1470, doi: [10.1029/97JD02929](https://doi.org/10.1029/97JD02929), 1998a.
- 794 Röckmann, T., Brenninkmeijer, C. A. M., Saueressig, G., Bergamaschi, P., Crowley, J. N.,  
795 Fischer, H., and Crutzen, P. J.: Mass-independent oxygen isotope fractionation in atmospheric CO as a  
796 result of the reaction CO+OH, *Science*, **281**, 544–546, doi: [10.1126/science.281.5376.544](https://doi.org/10.1126/science.281.5376.544), 1998b.
- 797 Röckmann, T., Jöckel, P., Gros, V., Bräunlich, M., Possnert, G., and Brenninkmeijer, C. A. M.: Using <sup>14</sup>C,  
798 <sup>13</sup>C, <sup>18</sup>O and <sup>17</sup>O isotopic variations to provide insights into the high northern latitude surface CO  
799 inventory, *Atmos. Chem. Phys.*, **2**, 147–159, doi: [10.5194/acp-2-147-2002](https://doi.org/10.5194/acp-2-147-2002), 2002.
- 800 Savarino, J., Bhattacharya, S. K., Morin, S., Baroni, M., and Doussin, J. F.: The NO+O<sub>3</sub> reaction: A triple  
801 oxygen isotope perspective on the reaction dynamics and atmospheric implications for the transfer of  
802 the ozone isotope anomaly, *J. Chem. Phys.*, **128**, 194303, doi: [10.1063/1.2917581](https://doi.org/10.1063/1.2917581), 2008.
- 803 Savarino, J. and Morin, S.: The N, O, S Isotopes of Oxy-Anions in Ice Cores and Polar Environments, in:  
804 Handbook of Environmental Isotope Geochemistry, edited by: Baskaran, M., Advances in Isotope  
805 Geochemistry, Springer Berlin Heidelberg, 835–864, 2012.
- 806 Scharffe, D., Slemr, F., Brenninkmeijer, C. A. M., and Zahn, A.: Carbon monoxide measurements onboard  
807 the CARIBIC passenger aircraft using UV resonance fluorescence, *Atmos. Meas. Tech.*, **5**, 1753–1760,  
808 doi: [10.5194/amt-5-1753-2012](https://doi.org/10.5194/amt-5-1753-2012).
- 809 Schinke, R., Grebenshchikov, S. Y., Ivanov, M. V., and Fleurat-Lessard, P.: Dynamical Studies Of The  
810 Ozone Isotope Effect: A Status Report, *Annu. Rev. Phys. Chem.*, **57**, 625–661,  
811 doi: [10.1146/annurev.physchem.57.032905.104542](https://doi.org/10.1146/annurev.physchem.57.032905.104542), 2006.
- 812 Stevens, C. M., Kaplan, L., Gorse, R., Durkee, S., Compton, M., Cohen, S., and Bielling, K.: The Kinetic  
813 Isotope Effect for Carbon and Oxygen in the Reaction CO+OH, *Int. J. Chem. Kinet.*, **12**, 935–948,  
814 doi: [10.1002/kin.550121205](https://doi.org/10.1002/kin.550121205), 1980.
- 815 Vicars, W. C., Bhattacharya, S. K., Erbland, J., and Savarino, J.: Measurement of the <sup>17</sup>O-excess ( $\Delta^{17}\text{O}$ ) of  
816 tropospheric ozone using a nitrite-coated filter, *Rapid Commun. Mass Spectrom.*, **26**, 1219–1231,  
817 doi: [10.1002/rcm.6218](https://doi.org/10.1002/rcm.6218), 2012.
- 818 Vicars, W. C. and Savarino, J.: Quantitative constraints on the <sup>17</sup>O-excess ( $\Delta^{17}\text{O}$ ) signature of surface  
819 ozone: Ambient measurements from 50°N to 50°S using the nitrite-coated filter technique,  
820 *Geochim. Cosmochim. Acta*, **135**, 270–287, doi: [10.1016/j.gea.2014.03.023](https://doi.org/10.1016/j.gea.2014.03.023), 2014.
- 821 Zahn, A., Brenninkmeijer, C. A. M., Maiss, M., Scharffe, D. H., Crutzen, P. J., Hermann, M.,  
822 Heintzenberg, J., Wiedensohler, A., Güsten, H., Heinrich, G., Fischer, H., Cuijpers, J. W. M., and van  
823 Velthoven, P. F. J.: Identification of extratropical two-way troposphere-stratosphere mixing based on  
824 CARIBIC measurements of O<sub>3</sub>, CO, and ultrafine particles, *J. Geophys. Res.*, **105**, 1527–1535,  
825 doi: [10.1029/1999jd900759](https://doi.org/10.1029/1999jd900759), 2000.
- 826 Zahn, A., Brenninkmeijer, C. A. M., Asman, W. A. H., Crutzen, P. J., Heinrich, G., Fischer, H.,  
827 Cuijpers, J. W. M., and van Velthoven, P. F. J.: Budgets of O<sub>3</sub> and CO in the upper troposphere:

828 CARIBIC passenger aircraft results 1997–2001, *J. Geophys. Res. Atm.*, **107**, 4337,  
 829 doi: [10.1029/2001jd001529](https://doi.org/10.1029/2001jd001529), 2002.

830 Zahn, A., Weppner, J., Widmann, H., Schlote-Holubek, K., Burger, B., Kühner, T., and Franke, H.: A fast  
 831 and precise chemiluminescence ozone detector for eddy flux and airborne application,  
 832 *Atmos. Meas. Tech.*, **5**, 363–375, doi: [10.5194/amt-5-363-2012](https://doi.org/10.5194/amt-5-363-2012), 2012.

833

834 **Tables**

835 Table 1. Ozone  $^{18}\text{O}/^{16}\text{O}$  isotope ratios from literature and this study

Domain	T (K)	P (hPa)	$\delta^{18}\text{O}(\text{O}_3)$ (‰)	Remarks
Stratosphere	190–210	13–50	83–93 (<3)	1
UT/LMS	220–235	240–270	89–95 (8)	2
			84–88 (6)	T
			91–98 (9)	TC
			112–124 (17)	C
Laboratory	190–210	67	87–97 (6)	3
	220–235	67	102–110 (6)	3
	220–235	240–270	95–103	4

Notes: Values in parentheses denote the average of the estimates' standard errors. The expected  $\text{O}_3$  isotope composition

on the VSMOW scale is calculated from the  $\text{O}_3$  enrichments reported relative to  $\text{O}_2$  using  $\delta^{18}\text{O}(\text{O}_3)_{\text{VSMOW}} =$   
 $\delta^{18}\text{O}(\text{O}_2)_{\text{VSMOW}} + \frac{18}{16} \delta^{18}\text{O}(\text{O}_3)_{\text{Air-O}_2} + [\delta^{18}\text{O}(\text{O}_2)_{\text{VSMOW}} \times \frac{18}{16} \varepsilon(\text{O}_3)_{\text{Air-O}_2}]$ .

<sup>1</sup> Observations (see Krankowsky *et al.* (2007) and refs. therein), lowermost values (19–25 km). Quoted temperature range is derived by matching measured  $\delta^{18}\text{O}(\text{O}_3)$  and laboratory data (see note <sup>3</sup>).

<sup>2</sup> This study, C1 observations (10–12 km). Letters denote the estimates derived using the data from Bhattacharya *et al.* (2008) and assuming only terminal (T), only central (C) and equiprobable terminal and central (TC)  $\text{O}_3$  atoms transfer to the artefact  $\text{CO}$ .

<sup>3</sup> Calculated using the laboratory KIE temperature dependence data summarised by Janssen *et al.* (2003).

<sup>4</sup> Calculated assuming a pressure dependence of the  $\text{O}_3$  formation KIE similar to that measured at 320 K (see Guenther *et al.* (1999) and refs. therein).

Deleted: ~

Deleted: ~

Deleted: -

Deleted: ε

Deleted: .

Deleted: .

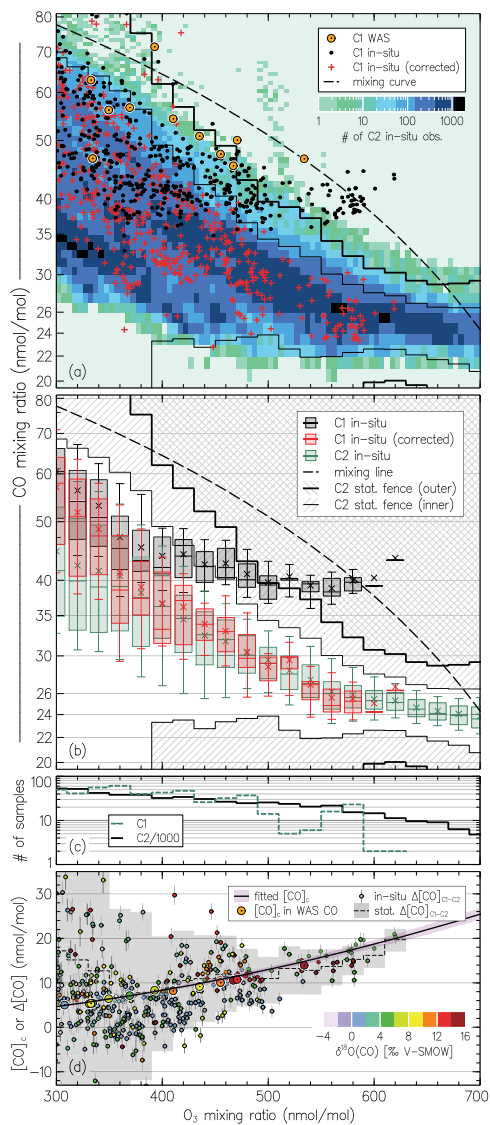
Deleted: ε

Deleted: 2

Deleted: .

Deleted: 2

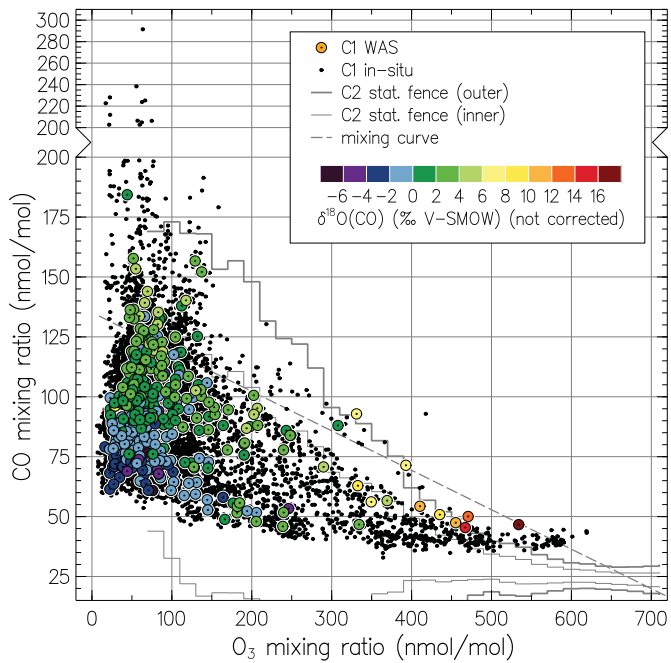




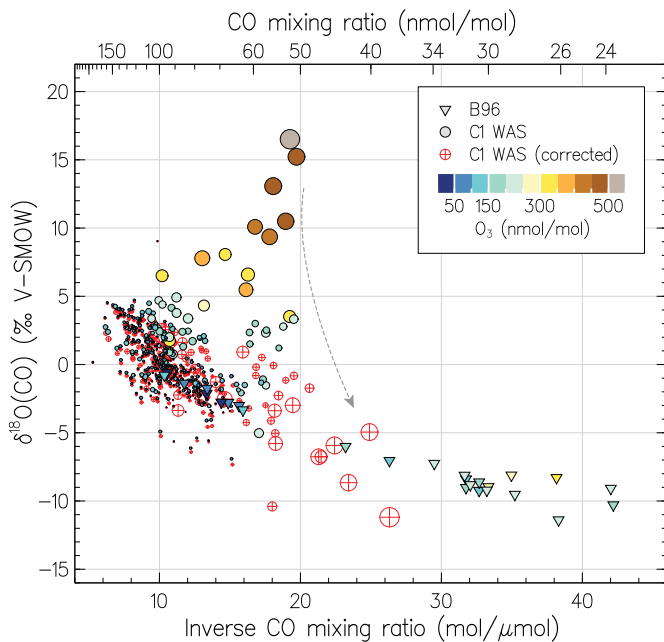
837 Fig. 1. (a) Distribution of CO mixing ratios as a function of concomitant O<sub>3</sub> mixing ratios measured by  
838 CARIBIC in the LMS ([O<sub>3</sub>] > 300 nmol/mol). The shaded area is the two-dimensional histogram of the C2  
839 measurements (all C2 data obtained until June 2013) counted in 5 × 1 nmol/mol size [O<sub>3</sub>] × [CO] bins, thus  
840 darker areas emphasise greater numbers of particular CO–O<sub>3</sub> pairs observed. Small symbols denote the  
841 original C1 *in situ* measurements (black) and corrected for the artefacts (red); the C1 WAS analyses (11 of  
842 total 408) are shown with large symbols. Thin and thick step-lines demark the inner and outer statistical  
843 fences (ranges outside which the data points are considered mild or extreme outliers, see text) of the C2  
844 data, respectively. The dashed curve exemplifies compositions expected from the linear mixing of very  
845 different (*e.g.*, tropospheric and stratospheric) end-members. (b) Statistics on CO mixing ratios from C1  
846 and C2 data shown in box-and-whisker diagrams for samples clustered in 20 nmol/mol O<sub>3</sub> bins (whiskers  
847 represent 9<sup>th</sup>/91<sup>st</sup> percentiles). (c) Sample statistic for each CARIBIC dataset (note the C2 figures scaled  
848 down by a factor of 1000). (d) Estimates of the C1 *in situ* CO contamination strength  $[CO]_c$  as a function  
849 of [O<sub>3</sub>] (solid line) obtained by fitting the difference  $\Delta[CO]$  between the C2 and C1 *in situ* [CO] (small  
850 symbols) as detailed in Appendix A<sub>v</sub> (Eq. (A1)). Step line shows the  $\Delta[CO]$  for the statistical averages (the  
851 shaded area equals the height of the inner statistical fences of the C2 data). Large symbols denote the estimates  
852 of  $C_c$  in the C1 WAS data (slight variations *vs.* the *in situ* data are due to the sample mixing effects, see Sect. 3). Colour denotes the respective C1 WAS  $\delta^{18}O(CO)$  (note that typically 6–7 *in situ* measurements correspond to one WAS sample).

Deleted: in the kinetic framework (see

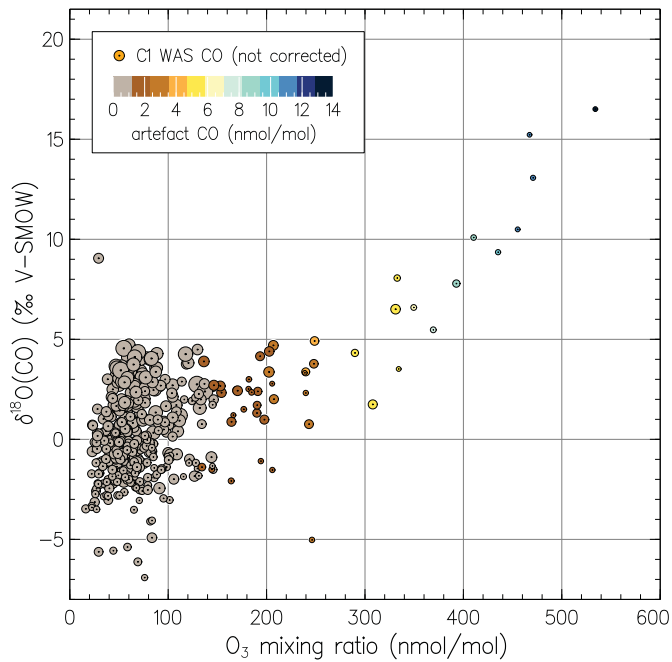
Deleted: ,



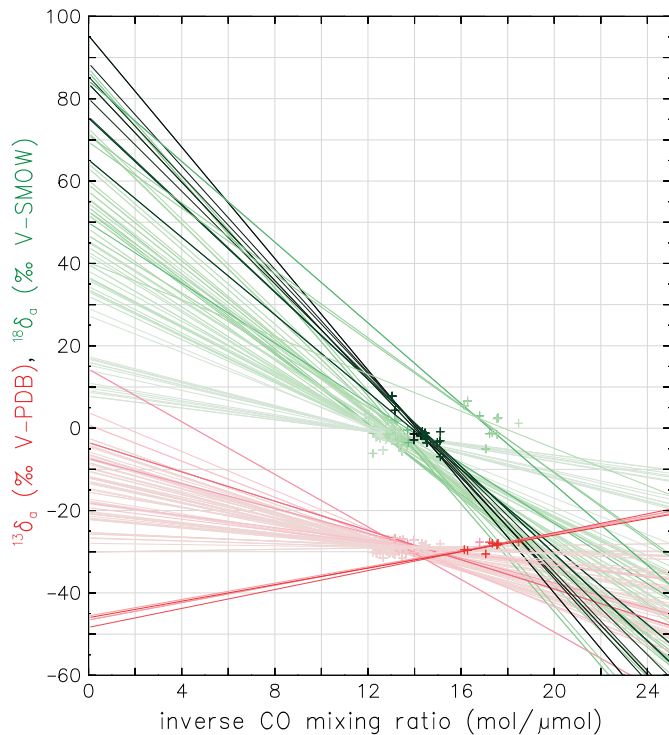
857 Fig. 2. (accompanies Fig. 1) Carbon monoxide and ozone mixing ratios measured in C1. Small black sym-  
 858 bols denote the C1 *in situ* measurements ( $n = 12753$ ). The C1 WAS analyses ( $n = 408$ ) are shown with  
 859 large symbols; colour denotes the concomitant  $\delta^{18}\text{O}(\text{CO})$  measurements. Thin and thick step-lines denote  
 860 the inner and outer statistical fences of the C2 data, respectively. The dashed curve exemplifies composi-  
 861 tions expected from the linear mixing of tropospheric and stratospheric end-members (see caption to Fig. 1  
 862 for details).



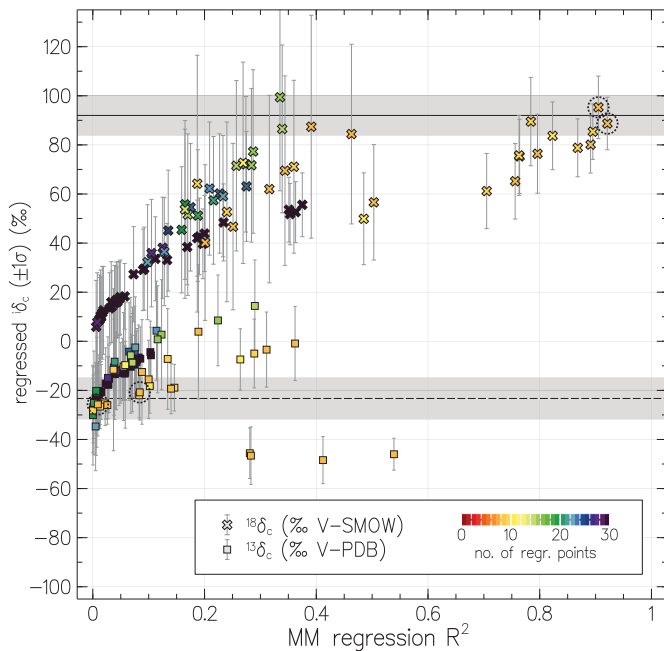
863 Fig. 3.  $^{18}\text{O}/^{16}\text{O}$  isotope composition of CO as a function of its reciprocal mixing ratio. Triangles present  
 864 the data from the remote SH UT/LMS obtained by Brenninkmeijer *et al.* (1996) (B96). Colour refers to the  
 865 concomitantly observed  $\text{O}_3$  abundances; note the extremely low  $[\text{O}_3]$  encountered by B96 in the Antarctic  
 866 "ozone hole" conditions. Filled and hollow circles denote the original and corrected (as exemplified by the  
 867 dashed arrow) C1 WAS data, respectively, with the symbol size scaling proportional to the estimated con-  
 868 tamination magnitude (see text).



869 Fig. 4. Measured C1 WAS  $\delta^{18}\text{O}(\text{CO})$  (not corrected for artefacts) as a function of concomitant  $\text{O}_3$  mixing  
 870 ratio. Symbol colour denotes the artefact CO component (integral  $[\text{CO}]_e$  per each WAS); symbol size  
 871 scales proportionally to the WAS CO mixing ratio corrected for artefacts (see Sect. 3 for details).

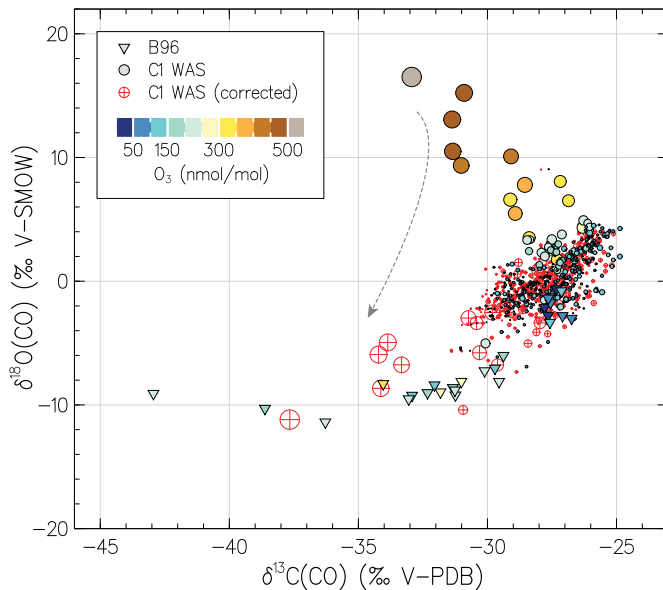


872 Fig. 5. Keeling plot of the data used in the calculations with the mixing model (MM). The C1 WAS iso-  
 873 tope CO measurements are shown with symbols, solid lines denote the linear regressions through the vari-  
 874 ous sets of samples selected by the MM ( $n = 80$  sets are plotted). Colours refer to the  $\delta^{13}\text{C}$  (red) and  $\delta^{18}\text{O}$   
 875 (green) data, colour intensity indicates the coefficient of determination ( $R^2$ ) of each regression, respective-  
 876 ly. Darker colours denote higher  $R^2$  values, with maxima of 0.92 for  $\delta^{18}\text{O}$  and 0.54 for  $\delta^{13}\text{C}$  data, respec-  
 877 tively. The inferred contamination signatures ( $\delta_c$ ) are found at  $([\text{CO}]_a)^{-1} \rightarrow 0$ . Regression uncertainties are  
 878 shown in Fig. 6. Note that because different subsets of samples contain same data points, some of the  
 879 symbols are plotted over (*i.e.*, not all symbols contributing to a particular regression case may be seen).



880 Fig. 6. Results of the regression calculation with the MM. Shown with symbols are the contamination  
 881 source isotope signatures  $\delta_c$  as a function of the respective coefficient of determination ( $R^2$ ). Colour de-  
 882 notes the number of samples in each subset selected. Solid and dashed lines present the best guess  
 883  $\pm 1$  standard deviation of the mean for the  $^{18}\text{O}$  and  $^{13}\text{C}$  estimates. Dashed circles mark the estimates ob-  
 884 tained at highest  $R^2$  for  $^{13}\text{C}$  regression (above 0.9). See text for details.

- Deleted:  $\delta^{18}\text{O}(\text{O}_2)$
- Deleted:  $\delta^{13}\text{C}(\text{C}_c)$
- Deleted: values
- Deleted:  $^{18}\text{O}$
- Deleted:  $r$



890 Fig. 7.  $^{18}\text{O}/^{16}\text{O}$  and  $^{13}\text{C}/^{12}\text{C}$  isotope composition of CO measured in C1. Triangles present the data from the  
 891 remote SH UT/LMS obtained by Brenninkmeijer *et al.* (1996) (B96). Colour refers to the concomitantly  
 892 observed  $\text{O}_3$  abundances; note the extremely low  $[\text{O}_3]$  encountered by B96 in the Antarctic ozone-hole  
 893 conditions. Filled and hollow circles denote the original and corrected (as exemplified by the dashed ar-  
 894 row) C1 WAS data, respectively, with the symbol size scaling proportional to the estimated contamination  
 895 magnitude (see text for details).



s  $K$  and  $\kappa$  describes the stoichiometry of the system with respect to ozone, *i.e.* how many (rate-determining) reactions of  $X$  and  $O_3$  ((with the individual unknown rate coefficients  $^X k_r$  and  $^{O_3} k_r$  or its derivatives)) may have lead to production of one artefact CO, respectively. The yield  $\lambda_{O_3}$ , a diagnostic quantity, relates the amount of artefact CO molecules produced to the total number of  $O_3$  molecules consumed in the system. Based on Eq. (A1), the functional dependence of the artefact CO component (denoted  $[CO]_c$ , obtained by discriminating the C1 outliers from respective C2 data) on  $[O_3]$  or  $[X]$  is generally formulated as (abundances in number density units are used)

$$C_c = \int_{\tau_c}^t \prod_{\kappa}^{O_3} k_r [O_3] \prod_K^X k_r [X] dt, \quad (A2)$$

where  $\tau_c$  denotes the contamination reaction time.

[1]

,  $K$  and  $[X]$  (the latter was chosen iteratively from a set of carbonaceous species measured). Practically, however, this regression analysis ascertains that variations in  $[CO]_c$  are exhaustively described using  $[O_3]$  and  $\kappa$ . Furthermore, we find that no other species or operational parameter (e.g. temperature, pressure, flight duration, latitude, etc.) measured in C1 appear to determine (correlate with)  $[CO]_c$ . Based on this, we can reduce Eq. (A2) to its final, simpler form, viz.

$$[CO]_c = \lambda_{O_3} k_c [O_3]^\kappa \tau_c, \quad (A3)$$

where  $k_c$  denotes the overall pseudo-first-order rate coefficient of the reaction chain that is exclusively propelled by  $O_3$ . The product  $(\lambda_{O_3} k_c \tau_c)$  thus integrates the influence of the unknown (and likely invariable)  $[X]$ ,  $^X k_r$ ,  $K$  and  $\tau_c$

[2]

the product  $(\lambda_{O_3} k_c \tau_c)$  that proportionates the CO contamination strength and  $[O_3]$  is found to be

[3]